THE REPUBLIC OF TÜRKİYE

MUĞLA SITKI KOÇMAN UNIVERSITY

GRADUATE SCHOOL OF NATURAL AND APPLIED SCIENCES

DEPARTMENT OF GEOLOGICAL ENGINEERING

DETERMINATION OF MICROPLASTICS AND NANOPLASTICS IN SATURATED POROUS MEDIA

MASTER OF SCIENCE THESIS

SELÇUK ORAL

SEPTEMBER 2023

MUĞLA

THE REPUBLIC OF TÜRKİYE

MUĞLA SITKI KOÇMAN UNIVERSITY

GRADUATE SCHOOL OF NATURAL AND APPLIED SCIENCES

DEPARTMENT OF GEOLOGICAL ENGINEERING

DETERMINATION OF MICROPLASTICS AND NANOPLASTICS IN SATURATED POROUS MEDIA

MASTER OF SCIENCE THESIS

SELÇUK ORAL

SEPTEMBER 2023

MUĞLA

MUĞLA SITKI KOÇMAN ÜNİVERSİTESİ

Graduate School of Natural and Applied Sciences

APPROVAL OF THE THESIS

The thesis submitted by SELÇUK ORAL with the title of "**DETERMINATION OF MICROPLASTICS AND NANOPLASTICS IN SATURATED POROUS MEDIA**" has been unanimously/majority accepted by the jury members to fulfill the requirements for the necessary conditions for master degree of Department of Geological Engineering at 29/09/2023

THESIS DEFENCE JURY

Assoc. Prof. Dr. Bedri KURTULUŞ (Supervisor) Signature:
Department of Geological Engineering,
Muğla Sıtkı Koçman University, Muğla _____

Prof. Dr. Philippe Le Coustumer (Member) Signature:
CNRS-INRAE-INSERM, Bordeaux Imaging Center,
University of Bordeaux _____

Prof. Dr. Frédéric HUNEAU (Member) Signature:
Faculty of Science and Technique,
University of Corsica Pasquale Paoli _____

APPROVAL OF HEAD OF THE DEPARTMENT

Prof. Dr. Semih GÜRSU Signature:
Head of Geological Engineering Department,
Muğla Sıtkı Koçman University, Muğla _____

Assoc. Prof. Dr. Bedri KURTULUŞ (Supervisor) Signature:
Department of Geological Engineering,
Muğla Sıtkı Koçman University, Muğla _____

Date: 29/09/2023

I hereby declare that all information in this document has been obtained and presented by academic rules and ethical conduct. I also declare that, as required by these rules and conduct, I have fully cited and referenced all material and results that are not original to this work.

Selçuk ORAL

29/09/2023

ABSTRACT

DETERMINATION OF MICROPLASTICS AND NANOPLASTICS IN SATURATED POROUS MEDIA

SELÇUK ORAL

Master of Science (M.Sc.)

Graduate School of Natural and Applied Sciences

Department of Geological Engineering

Supervisor: Assoc. Prof. Dr. Bedri KURTULUŞ

September 2023, 54 Pages

Unavoidably the extensive usage of artificially manufactured nanoplastics or microplastics in everyday life products leads to their release to the terrestrial environments as well as aquatic environments. Besides their impact on the public health, they are also threatening environment. In this study, with regard to environmental influences, it was aimed to understand how it behaves and its effects porosity in saturated porous environments. Different types and concentrations and their effects were investigated by examining quartz sand samples which was used and collected from 1D plastics transfer column experiments. Collected quartz sand samples were imaged in Scanning Electron Microscopy (SEM) to observe attached nanoplastics on the grain surface of quartz sand. BET surface area analysis method was used to observe the surface area changement of the contaminated sand samples by NPls in different concentrations and revealed that, surface area can increase up to 41%. Mercury (Hg) porosimetry method also was used to analyze and compare the porosity changement between contaminated samples and initial conditions. It was revealed that unporous quartz sand samples were not suitable to do this analyzes. Other quartz sand sample which has rougher surface and irregularities has revealed that depends on concentrations porosity can decrease up to %22. As a complimentary method, raw and contaminated sand samples was observed with X-ray tomography method and with the same trend, porosity was found lower in contaminated sand against to raw sample. This study was shown nano and microplastics has negative effect on material in the terms of porosity.

Keywords : Nanoplastic, Microplastic, Sand, TEM, SEM, Hg Porosimetry, BET Analysis

ÖZET

DOYGUN GÖZENEKLİ ORTAMDA MİKROPLASTİKLER VE NANOPLASTİKLERİN BELİRLENMESİ

Selçuk ORAL

Yüksek Lisans Tezi

Fen Bilimleri Enstitüsü

Jeoloji Mühendisliği Anabilim Dalı

Danışman: Doç. Dr. Bedri KURTULUŞ

Eylül 2023, 54 Sayfa

Yapay olarak üretilen nanoplastiklerin veya mikroplastiklerin günlük yaşam ürünlerinde yaygın kullanımı, kaçınılmaz olarak karasal ortamlara ve su ortamlarına salınmalarına yol açmaktadır. Bu plastiklerin halk sağlığı üzerindeki etkilerinin yanı sıra, çevreyi de tehdit etmektedirler. Bu çalışmada, çevresel etkiler açısından, doymuş gözenekli ortamlarda nasıl davrandığının ve gözenekliliğe etkilerinin anlaşılması amaçlanmıştır. Farklı tip ve konsantrasyonlar ile etkileri, 1D plastik transfer kolonu deneylerinden kullanılan ve toplanan kuvars kumu örnekleri incelenerek araştırılmıştır. Toplanan kuvars kumu örnekleri, kuvars kumunun tahıl yüzeyine bağlı nanoplastikleri gözlemlemek için Taramalı Elektron Mikroskobu'nda (SEM) görüntülendi. Kirlenmiş kum numunelerinin yüzey alanı değişimini farklı konsantrasyonlarda NPls ile gözlemlemek için BET yüzey alanı analiz yöntemi kullanılmış ve yüzey alanının %41'e kadar yükselebildiği ortaya çıkmıştır. Kontamine numuneler ile başlangıç koşulları arasındaki gözeneklilik değişimini analiz etmek ve karşılaştırmak için cıva (Hg) porosimetri yöntemi de kullanılmıştır. Gözeneksiz kuvars kumu numunelerinin bu analizleri yapmaya uygun olmadığı ortaya çıkmıştır. Daha pürüzlü yüzeye ve düzensizliklere sahip diğer kuvars kumu numunesi, konsantrasyonlara bağlı olarak gözenekliliğin %22'ye kadar azalabildiğini ortaya koymuştur. Tamamlayıcı bir yöntem olarak X-ışını tomografi yöntemi ile ham ve kontamine kum örnekleri gözlenmiş ve aynı eğilim ile kontamine kumda ham numuneye göre gözeneklilik daha düşük bulunmuştur. Bu çalışmada nano ve mikroplastiklerin gözeneklilik açısından malzeme üzerinde olumsuz etkileri olduğu gösterilmiştir.

Anahtar Kelimeler: Nanoplastik, Mikroplastik, Kum, TEM, SEM, Hg Porozimetri BET Analizi

To my lovely family, who always supports and encourages me adorably.

ACKNOWLEDGEMENT

First of all sincerely I would like express my appreciation to my supervisor Assoc. Prof. Bedri KURTULUŞ and Prof. Dr. Philippe Le COUSTUMER for their guidance, effort and patient.

I am extremely grateful to Muğla Sıtkı Koçman Foundation and French Embassy Ankara for their financial support on this study.

I would like to thank BORDEAUX IMAGING CENTER and ENSEGID for the laboratory facilities and specially I would like to acknowledge the assistance Lea PIGOT, Serge GALAUP and Hande OKUTAN for their all support.

I would like to express my deepest gratitude to Betül ŞENTÜRK for all the support and patience that cannot be underestimated.

Lastly, many thanks to my adorable family for believing in me and their endless support.

TABLE OF CONTENT

LIST OF FIGURES

LIST OF TABLES

LIST OF ABBREVIATIONS

µm : Micrometer

nm : Nanometer

mm : Millimeters

mg : Milligram

cm: Centimeter

l : Liter

MPls : Microplastics

NPls : Nanoplastics

TEM: Transmission Electron Microscopy

SEM: Scanning Electron Microscopy

PE: Polyethylene

PS: Polystyrene

Aoi : Area of Interest

1. INTRODUCTION

Every year, plastic consumption increases all over the world and as indicated by Macleod et al., (2021) as of 2016, estimates of plastic trash emissions into rivers, lakes, and the ocean range from 9 to 23 million metric tons annually whereas for emissions into the terrestrial environment, they range from 13 to 25 million metric tons annually and according to scenarios based on business as usual, these projected emission rates for 2016 will have about quadrupled by 2025. With the increase, scientific researches on environmental pollution has become increasingly popular due to its harmful side effects (McDevitt et al., 2017). In the study of Ahamada and Doğruöz (2020) mentioned that human is affected by environmental microplastic pollution and furthermore, they indicated that 83% of 159 drinking water samples from five continents have been found contaminated with microplastics and they clarify that the understanding of how plastics affect ecosystems indicates these pollutants may have harmful impacts when present as both small and large particles. As plastic utilization with all aspects of life and then breaks into smaller particles, there is a global concern over possible impacts on human health and the environment caused by microplastics (MPls) or nanoplastics (NPls) (Yee et al., 2021). Due to their ability to adsorb contaminants including heavy metals and persistent organic pollutants, plastic particles are now widely acknowledged to pose dangers to both the natural ecosystem and human health (He et al., 2018). The classification of plastic size may vary depending on the study. In the study of Mariano et al., (2021), microplastics defines as particles smaller than 5 mm whereas nanoparticles define with a range size from 1 nm to 1 μm.

Porous media can be considered as a bridge between surface and subsurface media and as defined by Leon, (1998) the percentage of empty space in a solid is known as its porosity and a porous media is a solid or group of solid bodies that have enough free space within or around them for a fluid to travel through or around them is referred to as a porous medium. As indicated by Alshehrei, (2017), with the lack of effective procedures to ensure the safe disposal of those plastics, its ends up with accumulate

these tiny particles in porous media such as soil, sediments. Our knowledge of how plastics affect ecosystems suggests that these pollutants may have harmful impacts when present as both small and large fragments. However, information on the type and extent of damage caused by tiny plastic particles at environmentally relevant concentrations is still limited (Windsor et al., 2019). Plastic contamination in terrestrial habitats has not attracted as much attention as it has in marine environments up until lately. In actuality, terrestrial ecosystems serve as an even greater sink for plastics. Yu & Flury, (2021) indicated that lands receive 4-23 times more plastic than oceans do and they furtherly mentioned that plastics enter terrestrial habitats by trash, air deposition, irrigation and flooding, agricultural mulching, and application of compost and sewage sludge. According to Chia et al., (2021), NPls and MPls may eventually find their way into water when they are dumped in a terrestrial environment. While some of these tiny plastic particles may eventually go vertically into the subsoil and/or enter the groundwater system via porous media. The introduction of microplastics into the groundwater system may have negative effects on the environment, human health, and plant, animal, and microbial life.

In the literature there is a few research on the topic of transport of microplastics in saturated porous media as in knowledge of author. He et al., (2018) have studied of plastic particles on the transport, deposition from the nano size to micro size particles and have shown that at high ionic strength conditions increases bacterial transport more than low ionic strength in quartz sand porous medium. Experimental study of Yu & Flury (2021) on current understanding of subsurface transport of micro and nanoplastics in soil mentioned that microplastics and nanoplastics can enter the soil as primary or secondary plastic particles, and their movement is influenced by their colloidal and surface properties, which are greatly influenced by their intrinsic qualities and subsequent environmental alterations. Additionally, soil texture and plastic qualities have a role in how micro and nanoplastics affect soil hydraulic properties. Insufficient experimental evidence is available to draw firm conclusions regarding how micro and nanoplastics affect the hydraulic characteristics of soils. Okutan et al., (2022) have carried out with the 1D column transport experiments with microplastics and fluorescent tracers in different saturated porous environments such as coarse size gravel, large silica small silica and sand media and it is discovered that the mean velocity is a crucial factor in the movement of polyethylene (PE) MPls

particles through a saturated porous medium. To have a better understanding of how presence of microplastics affect the transport of antibiotics, Hu et al., (2021) has shown that the presence of microplastics would change both the sorption rate and the transport rate of antibiotics, thus affecting its migration in saturated porous media, hence, microplastics in soil and sediments can retard the transport of useful antibiotics in saturated porous media by conducting column transfer experimental setup.

On the other hand, a geological factor called linked porosity (open porosity) can greatly influence the fluid storage and conducting capacity of rocks in addition to their mechanical characteristics. This has significant implications for the containment of hazardous material in the earth's subsoil (Klobes et al., 1997). Determination of porosity using Hg (mercury) porosimetry method and surface area analysis using for BET (Brunauer–Emmett–Teller) method analysis with different types of quartz sand material has been studied in previous research.Dong et al., (2018) has carried out the Hg porosimetry analysis with the different size of quartz sand and have found out that when the mercury pressure increased, the sample size effect to the measurements was decreased. Information on the type and extent of damage caused by tiny plastic particles at environmentally relevant concentrations is still limited. In the study of Hlaváč et al., (2014), photoactive quartz sand/titanium dioxide composite were prepared and the surface area analysis of quartz sand after and before the composites prepared in a part of this study was examined using the BET method and comparisons were made and the comparison of pure quartz sand and quartz sand samples with other samples which includes prepared composite were done. Brantley & Mellott (2022), in order to investigate controls on quantifying mineral-water reaction rates parameter for several primary silicate minerals specific surface area and porosity values of different types of primary silicate minerals were measured with BET surface area analysis method and other imaging methods and comparisons were made. Furthermore, Han et al., (2006) have done investigations of removal heavy metals in aquatic environments with mangan oxide coated sand and they used quartz sand samples and determine the characteristics and test the properties of prepared samples several imaging methods were used, they also made a comparison of surface area values for raw quartz sand samples with mixture included quartz sand samples. However, to the best of the author knowledge, there is no research to explore the behaviors of nanoplastics or not well

calibrated microplastics in saturated porous media, specifically on the sand grains in the frame of how its effect the porosity properties and surface area.

This study will be helpful to understand how different types of MPls and NPls effects porosity and surface area of materials with different concentration at the saturated porous media. In the study, two different types of silica quartz sand samples collected from one dimensional transport column test which used to explore transport microplastics and nanoplastics. After the characterizations of related MPls and NPls which was used in experiments, porosity measurements and surface area analysis were performed with collected sand samples to do a comparison between initial condition and contaminated sand sample

2. MATERIALS AND METHODS

2.1. Materials

MPls and NPls, which are intended for observation in saturated porous environments, have been acquired with different properties.

Polystyrene (PS) types of nanoplastic were used with two different surface functional groups and a cover. There are Amidine Polystyrene (APS), and Sulfate Polystyrene (SPS) which includes surface functional groups NPls and Sodium Dodecyl Sulfate covered Amidine Polystyrene (SDS). Ramirez Arenas et al., (2022) used similar types of NPls in their study and as they indicated in their study, PS types of NPls were provided by the Institute of Analytical Sciences (ISA) Micro & nanobiotechnology, University Claude Bernard Lyon, France whereas SPS was purchased from Invitrogen (ThermoFisher Scientific, Switzerland). As they determined by the TEM image analysis measurements and nanoplastics tracking analysis, their size was observed. These PS NPls mixtures were prepared and examined with pure water and a concentration of 50 mg/l. APS type surface functional group is positive charged where SPS is negative charged.

Polyethylene (PE) types of MPls were used in the microplastics-based experiments in this study. It was purchased from Goonvean Fibres in the solid powder format, white colored. It was indicated that it has size range between 0-30 μm. The size measurements were performed with optical microscopy image analysis to control the size distribution.

For the represent saturated porous media, two different kinds of sands were used. First is white colored named Turkish quartz sand which range size between 1.20 – 2.40 mm. It was provided by Esan Eczacıbaşı Industrial Raw Materials Industry and Commerce Inc as %99 silica sand. The SEM-EDX analysis were performed for investigation of atomic composition. Microplastic transport experiment has carried out with white Turkish sand and gray Geneva sand.

Second sand sample is gray colored named Geneva quartz sand sample. Geneva sand was charged negatively. Sand grains are classified into 11 granulometric classes and typically range in size from 2.38 to 2.83 mm, 2.83 to 3.36 mm, and 3.36 to 4.00 mm (Hul et al., 2022). Detailed table of it were given in appendix 1. It was provided by Carlo Bernasconi AG (Zürich, Switzerland). NPls based experiments were performed only with Geneva sand. The particle size measurements were done by imaging method to find size range and the size range was found 0.31 - 1.44 mm. Details can be seen in appendix 4.

Table 2.1. Usage of plastic types with porous media sand samples

Plastic Type	Sand Type	
	Geneva	Turkish
MPls	X	X
NPls	X	

The subject of this experimental study can be characterized as a sub-branch of column transport experiments. The samples examined within the scope of this study were produced from a different experimental study that will now be described. In that study, one-dimensional column experiments were performed to understand how microplastics behave in groundwater systems. In these one-dimensional transport column experiments, different injection suspensions which contains MPls and NPls of different sizes and concentrations were passed through columns filled with fully saturated sand. The experimental setup used for mentioned experimental study can be examined in Figure 2.1 below.

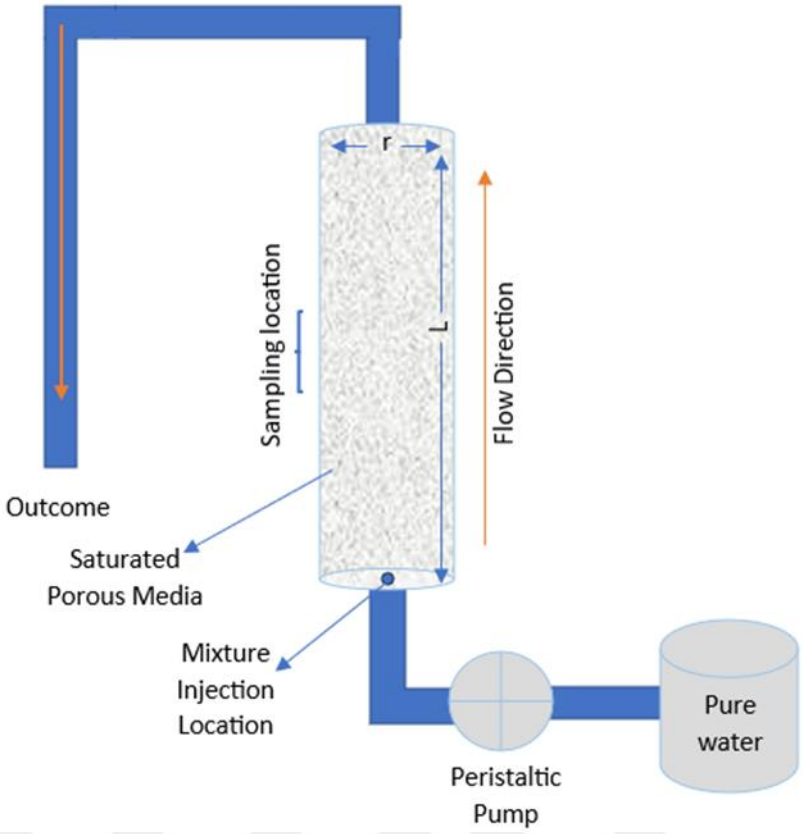

Figure 2.1. Experimental setup of transfer column tests

It based on experimental setup that can be seen above. As a property of setup, R value as a diameter of tube is equal to 3.6 cm and length of the column is 20 cm. Basically after the porous medium is saturated, artificially prepared mixture (which contained plastics surfactant with the ratio of 1:1 for MPls) with plastic and pure water are injected instantly from the bottom to the top of the vertical column with the help of a syringe. These injections were made with 0.3 ml and 0.5 ml injections depending on types of plastic used for each mixture.

In order to understand the how MPls and NPls behaves in the saturated porous media and investigate them on the notion of effects on porosity and surface area samples were collected from the saturated porous media after each column test experiment with different mixture of plastics within the tube to analyses. These samples were collected from the middle part of the saturated porous media column in the purpose of homogeneity or the best represent the circumstances. Each column test experiment workflow was first saturating the porous medium and then injecting the

mixture containing 0.3 ml of plastic for NPls based transfer column test experiments and 0.5 ml of plastic for MPls based transfer column test experiments.

These mixtures were prepared with different types of plastics with different types of surfactants in the pure water. Respectively, in order to do a decent comparison with affected samples, clean sample also were measured. This sample of clean sand is intended to represent the initial condition. To investigate how the porous media got affect by transport of NPls, with injection concentration 1000 mg/l, 500 mg/l and 100 mg/l variable concentration were prepared with pure water to inject to the saturated porous media. Sample list collected from NPls based experiments with the information of NPls types, sand sample name, injection concentrations list can be seen below in Table 2.2. Since only 0.3 ml prepared mixture was given to the saturated porous media, injected amounts and concentrations of injected NPls mixture were specified.

Table 2.2. Properties of collected samples from nanoplastics based experiment

Sand Type	Sample Name	Prepared mixture concentration (mg/l)	Used NPls types in the mixture	Injected mixture amount (ml)	Injected plastic Mass (g)
Geneva	GA1	0	Raw sample	0	0
Geneva	G2	1000	APS	0.3	0.3
Geneva	G4	100	APS	0.3	0.03
Geneva	G5	1000	SPS	0.3	0.3
Geneva	G7	100	SPS	0.3	0.03
Geneva	G8	1000	SDS	0.3	0.3
Geneva	G10	100	SDS	0.3	0.03

In order to perform MPls based transfer column test, also mixtures with different properties were prepared. The mixture was prepared with MPl with 1:1 ratio of surfactant. As a surfactant detergent was used which contains anionic surfactant. For the injection mixture surfactant was added. The 1:1 ratio of polyethylene microplastic-surfactant were used. As a surfactant, detergent containing anionic surfactant was used. Injection mixtures with a concentration of 20 g/l and 10 g/l were prepared. Sample list collected from microplastic based experiments with the information of microplastic types, sand sample name and type, injection concentrations list can be seen below in Table 2.3. Since only 0.5 ml prepared mixture was given to the saturated porous media,

injected mixture amount and concentration of injected microplastics with surfactant mixture were indicated in Table 2.3.

Table 2.3. Properties of collected samples from microplastic based experiment

Sand Type	Sample Name	Prepared mixture Concentration (g/l)	Used MPls types in the mixture	Injected Mixture Amount (ml)	Injected plastic Mass (g)
Geneva	GA1	0	Raw sample	0	0
Geneva	G11	20	PE + surfactant	0.5	0.01
Geneva	G12	10	PE + surfactant	0.5	0.005
Geneva	G13	10	PE + SDS surfactant	0.5	0.005
Turkish	T1	0	Raw sample	0.5	0
Turkish	T2	20	PE + surfactant	0.5	0.01
Turkish	T3	10	PE + surfactant	0.5	0.005

Sand samples were collected from plastic transport column experiments which has done under the conditions above with microplastics and nanoplastics. Collected samples were humid due to saturated media. So, each quartz sand sample were got dry in the oven under 40 °C minimum 24 hours before the relevant analysis if it was necessary. With those acquired samples were analyzed with different imaging instruments such as scanning electron microscopy (SEM), X-ray computed tomography and samples also were observed with Mercury (Hg) intrusion porosimetry and Brunauer–Emmett–Teller (BET) method.

2.2. Methods

2.2.1. Transmission electron microscopy (TEM)

The most popular method for analyzing nanomaterials in electron microscopy is transmission electron microscopy (TEM), which provides chemical data and images of materials with an atomic-scale spatial resolution (Mariano et al., 2021). This method is used to examine, surface imperfections or weaknesses, the atom's crystal structure, the size of the particle, and the composition of the sample. It was invented by Max Knoll and Ernst Ruska at Berlin in 1933 (Williams & Carter, 2009). Changing the magnification or focus is a necessary part of almost every TEM operation; electron

lenses are used to enlarge and focus the electron beam and the pictures. The restricted picture resolution in light microscopes, which is imposed by the wavelength of visible light, led to the development of TEMs historically. The realization that there are numerous other equally valid reasons for using electrons, the majority of which are used to some extent in a modern TEM, was made possible only after electron microscopes were invented (Williams & Carter, 2009).

An electron microscope is a microscope that enlarges images of samples by using an electron beam to illuminate the material. There are several components that all electron microscopes share. These elements typically include a pump assembly to maintain a proper vacuum in the microscopes' chambers, an electron source, electromagnetic lenses, a sample holding, and a detecting system. A sufficiently thin sample must be placed under an accelerated electron beam in order to perform transmission electron microscopy. A system of magnetic lenses is then used to project the transmitted image of the sample, which includes information about the sample's texture, onto a fluorescent screen, turning the electronic image into an optical one. The image may then be captured using a CDD (Charge-Coupled Device) and shown on a computer (Imaging Center Bordeaux, n.d.).

Figure 2.2. a - Hitachi - H7650 transmission electron microscope b- Object holder of TEM c - Electron microscopy carbon grid

Hitachi – H7650 transmission electron microscopy was used to image of APS, SDS, SPS nanoplastics containing mixtures which used in column experiments for instant injection to the saturated porous media. It is aimed to see the situation of nanoparticles before injection to the saturated porous media in the experimental setup. Size measurements were done after imaging. 50 mg/l concentrated pure water NPls mixtures was made. Each sample was put to sonic bath for 5 minutes to prevent any aggregation of particles. Afterward, the drop of mixture was dropped and dried on a copper-coated carbon mesh TEM grids under infrared lamp. Imaging was done with 80 kV or 120 kV accelerating voltage.

2.2.2. Scanning electron microscopy (SEM)

The SEM technique, often known as scanning electron microscopy, is extensively utilized across many academic fields. On a nanoscale to micrometer (nm– μm) scale, it can be regarded as an efficient approach for the analysis of organic and inorganic materials. With a high magnification up to 300,000x and even 1Mx (in some recent models), SEM reveals images of the texture of a variety of materials. Together with SEM, Energy Dispersive X-ray Spectroscopy (EDS) produces qualitative and semi-quantitative data. Together, the two methods have the ability to offer essential details on the material composition of scanned specimens that are not possible to obtain by standard laboratory assays. The EDS X-ray added the benefits of using a computer software to analyze the composition of numerous components in the sample. The latter speed up the entire process by converting the x-ray ratio's intensity to chemical compositions in a matter of seconds and improving the performance of quantitative analysis (Mohammed & Abdullah, 2018). Specimen is the placed material to microscope to observe. Because the specimen doesn't need to be made thin, the SEM has several advantages over a TEM, including the ease of specimen preparation. Actually, a lot of conducting specimens don't even need to be specifically cleaned up before SEM analysis (Egerton, 2005).

The basic concept of SEM has two main components which are an electron column and a control console. The electron column is made up of an electron gun, two or more electron lenses, and other components that affect the routes taken by electrons as they move down an evacuated tube. Vacuum pumps that generate a vacuum of about 10 Pa typically occupy the base of the column. The knobs and computer keyboard used to

control the electron beam are located next to a cathode ray tube (CRT) viewing screen in the control panel (Goldstein et al., 2003). When electron beam given from the top of electron column to the surface of interested material, secondary electrons and backscattered electrons reflects from the surface of material and many types of signals are generating. The signals are converted by the detector system's electronics into spot-by-spot intensity changes on the viewing screen, which create an image (Goldstein et al., 2003). In order to reach the best observation on imaging in SEM methods, it must prevent from electrostatic charging. Electrostatic charging could happen by two types, positive or negative. Negative charge present more serious problem as it deflects the scanning probe and repels the incident electrons, causing image distortion or variations in image intensity. To prevent this kind of charging problem, using the evaporation or sublimation method which done in the vacuum, surface of the material is coat with a thin film of metal or conducted carbon (Egerton, 2005). This method also increases conductivity and increases and facilitates electron reflection.

Figure 2.3 JSM-IT500 scanning electron microscope

JSM-IT500HR scanning electron microscopy was used to imaging the surface area of the quartz sand samples. Observation and imaging of nanoplastics or microplastics aggregations on the examined quartz sand grains were desired. It was aimed to investigate the surface micro textures of quartz sand samples, pores structure on the granular quartz sand grains. Also, X-EDS analysis methods were used to determine the atomic composition of Turkish sand grain. The quartz sand grains samples were replaced on the 12 mm diameter thick carbon adhesive tabs. Gold plating were done with EMSCOPE SC 500 and SB 250 metallizer to allow a good conductivity of the samples under the electron beam.

2.2.3. X-ray computed tomography

Over the past 15 years, X-ray computer tomography (CT) has had a period of rapid growth with notable advancements in spatial resolution and image reconstruction times, making it a widely used tool in materials labs (Maire & Withers, 2014). Tomographic analysis of samples of cooked materials involved scanning the material, analyzing digital images, and figuring out how much air was in each sample overall. After the object had completed a full 360 degrees of rotation, a series of images of the object were taken using a spatial X-ray beam and a panel detector. After pre-processing, the photos were combined to create a 3D model. The total number of projections generated for a full rotation determines how accurate the final projection is. Without damaging the samples, computed tomography enables analysis of their internal structure. With the help of this technique, a 3D image of the object's complete volume or a set of selected pieces can be created. Creating a tomographic image is based on measuring the absorption of radiation passing through an object (Stepien et al., 2022).

The object to be imaged is put in the X-ray beam's path, according to X-ray tomography principle. The transmitted X-rays are turned into visible light by a device called a scintillator, while some of the X-rays are absorbed. This light, which corresponds to a projection of the sample, is captured by a CCD (charge-coupled device) camera with the use of appropriate lenses. After that, the sample rotates by 180 or 360 degrees, and during this rotation, numerous projections - typically hundreds- are recorded. A 3D representation of the sample is recreated using this collection of projections, which is known as a scan. Typically, an optical or electronic microscope

is used to observe the microstructure and provide two-dimensional images. The accessible parameters in two dimensions have limits, and the methods used to create these images are frequently damaging to targeted sample. These two challenges may be solved thanks to X-ray microtomography. With a spatial resolution of the order of 1 µm, X-ray micro-tomography is an excellent tool for obtaining 3D data (Salvo et al., 2010). In several study fields, including soil science, hydrology, entomology, and material sciences, X-ray computed tomography offers plenty of possibilities for material research (Bulcke et al., 2009). Microstructural data acquisition with X-ray tomography can be used to observe porosity evolution on materials, grain size evolution, imaging the effects of substances on materials.

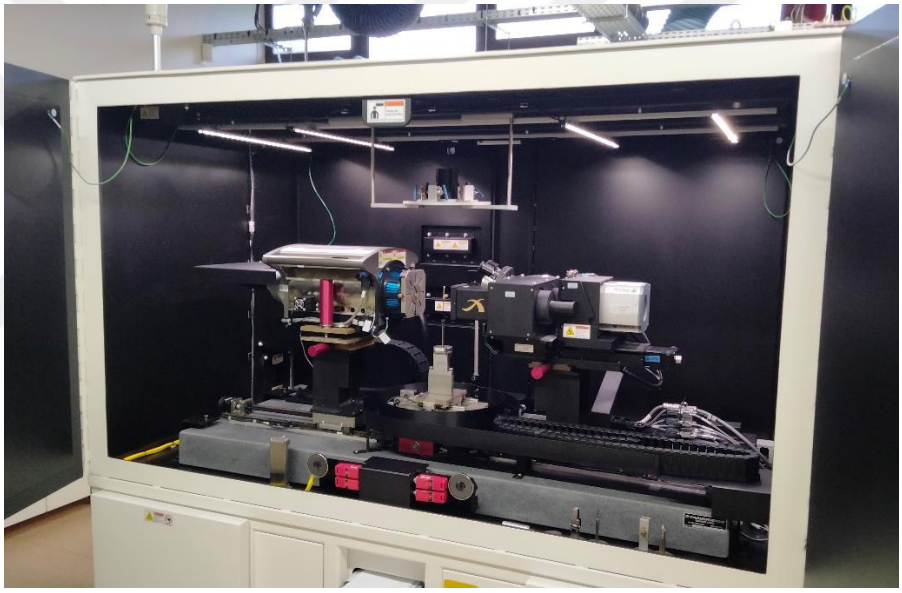

Figure 2.4. Zeiss -xradia 510 versa x-ray tomograph

Zeiss -Xradia 510 Versa brand x-ray computed tomography was used to imaging studied materials, quartz sand samples. In order to extract a faithful representation of the geometrical structure, or grain microstructure for numerical processing, visualize the arrangement of grains and to make data processing on porosity measurements this analysis was performed. The samples got dried 48 hours in the oven before being analyzed. Finally, the 3D images were done under the various amount accelerated voltage and energy to have higher or lower resolutions.

2.2.4. Brunauer-emmett-teller (bet) surface area analysis methods

The BET theory was created by Stephen Brunauer, Paul Emmett, and Edward Teller in 1938. In principle, the adherence of gas atoms or molecules to a surface is known as adsorption. The amount of gas adsorbed is influenced by the exposed surface area as well as by temperature, gas pressure, and the degree of gas-solid interaction. Nitrogen is frequently utilized in BET surface area analysis because it is easily accessible in high purity and interacts strongly with the majority of materials. In order to achieve measurable levels of adsorption, the surface is chilled using liquid N_2 because the contact between gaseous and solid phases is often minimal. The nitrogen gas is then delivered into the sample cell in known quantities. Pressure variations brought on by the adsorption process are monitored using highly accurate and precise pressure transducers. The sample is taken out of the nitrogen atmosphere once the adsorption layers have developed, which causes the adsorbed nitrogen to be released from the material and measured. A BET isotherm, which shows the quantity of gas adsorbed as a function of relative pressure, is used to display the collected data (Raja & Barron, 2022). This surface area is given in units of area/mass (e.g., m2/g) (Brame & Griggs, 2016).

The analysis is started after the sample to be analyzed is made the necessary operations. The analysis is simply; by supplying a known amount of nitrogen gas to the sample against time, providing a single-layer arrangement of nitrogen gas over the surface area of the sample and calculating from this how much surface area there is per unit weight.

BET equation, 1, uses the information from the isotherm to determine the surface area of the sample, where X is the weight of nitrogen adsorbed at a given relative pressure (P/P_0), X_m is monolayer capacity, which is the volume of gas adsorbed at standard temperature and pressure (STP), and C is constant. STP is defined as 273 K and 1 atm (Raja & Barron, 2022).

$$\frac{1}{X\left[\left(\frac{P_0}{P}\right)-1\right]} = \frac{1}{X_m C} + \frac{C-1}{X_m C}\left(\frac{P}{P_0}\right) \tag{2.1}$$

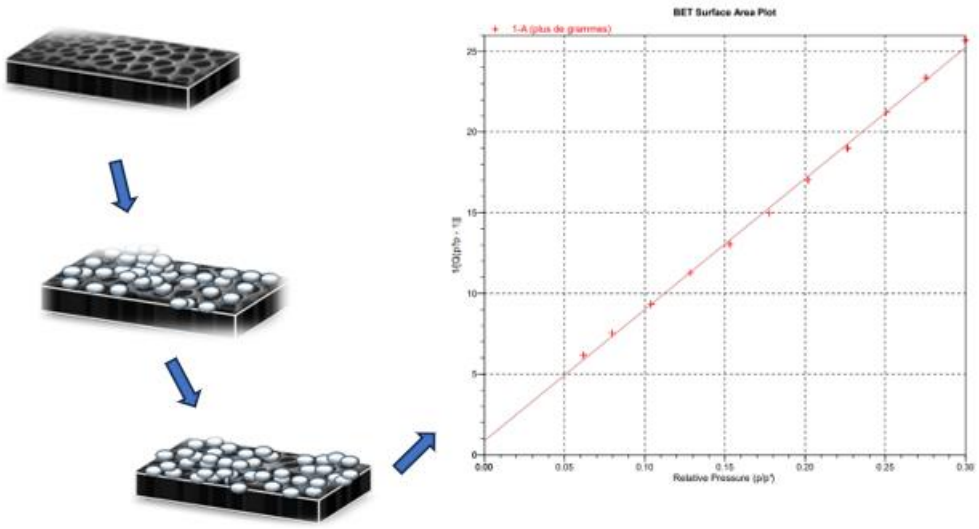

Figure 2.5. Bet surface area analysis illustration with nitrogen gas adsorption on the material surface and example surface area plot

BET equation, 1, requires a linear plot of 1/[X(P/P0)-1] against relative pressure (P/P0). From the definable slope (2), Intercept (3) and Weight of monolayer (4) values, Total surface area (S_t) can be derived by the formula 2.5.

$$S_t = \frac{C\ -1}{X_m C} \tag{2.2}$$

$$i = \frac{1}{X_m C} \tag{2.3}$$

$$X_m = \frac{1}{S_t + i} \tag{2.4}$$

The following equation (2.5), where LAV is Avogadro's number, Am is the cross sectional area of the adsorbate and equals 0.162 nm2 for an absorbed nitrogen molecule, can be used to compute the total surface area St once Xm has been established. Mv is the molar volume and equals 22414 ml.

$$S_t = \frac{X_m L_{av} A_m}{M_v} \tag{2.5}$$

When this method was used to determine the BET surface area of materials with both micro and mesopores, caution must be utilized because surface area measurement is impossible if pore condensation occurs within the chosen pressure range. The range

is between 0.2 nm to 80 nm for gas adsorption method as indicated by Schlumberger and Thommes, (2021) according to IUPAC (International Union for Pure and Applied Chemistry) standards.

Figure 2.6. Micromeritics asap 2020 surface area analysis instrument

Micromeritics ASAP 2020 surface area analyzer was used to investigate the surface area changement of granular quartz sand materials used in nanoplastic transfer column experiments with different concentration A sample of 10-11 grams of sand was used in each experiment for analysis. This technique and instruments were used only with samples which used for nanoplastic based experiments because due to application ranges is sensitive enough and suits to the size of NPls. Before each analysis, humid samples were got dried minimum 24 hours in 40 °C in oven and degassed with 8 hours vacuum in 40 °C.

2.2.5. Hg (mercury) intrusion porosimetry

Mercury porosimetry method, a widely used method for measuring pore structure (porosity, pore volume, and pore-throat size distribution) of reservoir rocks, can be utilized with a variety of sample sizes. In relation to pore connectivity, a rock sample may show sample size-dependent porosity; weakly linked rocks may have more porosity for smaller samples, and porosity reaches a stable value at particular sample sizes (Qiming and Qinhong, 2019). As stated by Rigby and Edler, (2002), the

characterization of porous media is frequently done using mercury porosimetry. For examining macroporous (pore sizes >50 nm) and larger mesoporous (2-50 nm) samples, it is frequently the method of choice. Mercury porosimetry is unique in that it covers a very wide range of pore sizes, including large pores (> 0.5 μm), which are difficult or impossible to probe reliably by other techniques. Mercury porosimetry is based on a simpler principle than alternative pore size characterization methods, which is the Washburn equations (2.6) (Leon, 1998).

$$p = -\frac{2\gamma \cos \theta}{r} \tag{2.6}$$

In the equations (2.6) where p is the imposed pressure (MPa), γ is the surface tension, θ is the contact angle of mercury and r is the radius of the pore (mm). Generally, in the use of equations the parameters γ and θ considered as a constant (Rigby & Edler, 2002). A clear and practical link between applied pressure and pore size is provided by the Washburn equation. In order to create pore size distributions, it is necessary to measure how much non-wetting mercury penetrates pores as a function of increasing applied pressure (Leon, 1998). Since mercury is a non-wettable liquid, it must be applied with the proper pressure in order for it to enter the sample's pores because it does not do so naturally. Mercury enters increasingly tiny pores as the set pressure rises. The measuring device calculates the volume and distribution of the pores based on the measured values of pressure and mercury intrusion into the sample (Stepien et al., 2022). Mercury porosimetry is, in theory, suitable to all types of solid materials. In practical circumstances, materials whose structure might compress or even collapse at high pressures need to have their compressibility corrected for or to be analyzed at low pressures (Leon, 1998).

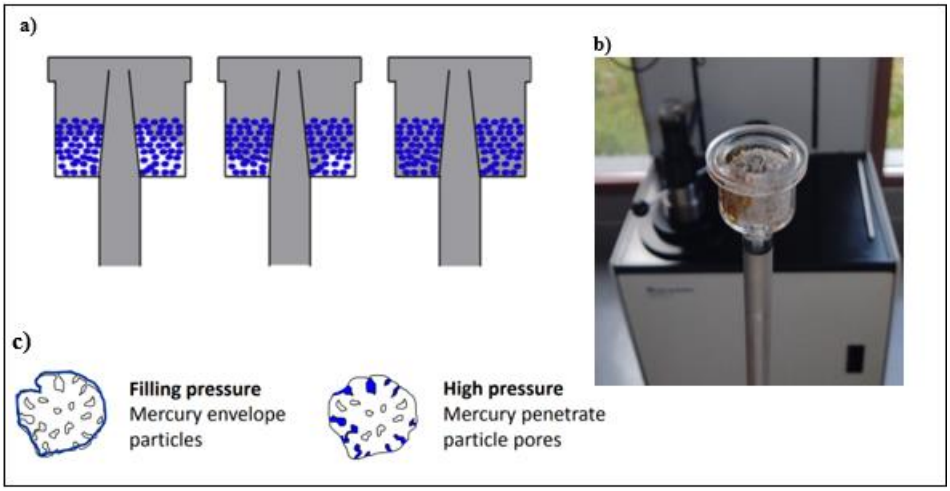

Figure 2.7. a - Illustration of interparticle voids filling with mercury in penetrometer b - penetrometer filled with granular quartz sand sample to being analyze c - illustration of filling interpores and intrapores

Mercury Intrusion Porosimetry can be applied to the materials which has pore size range between 5 nm -500000 nm as it indicated by Schlumberger and Thommes, (2021).

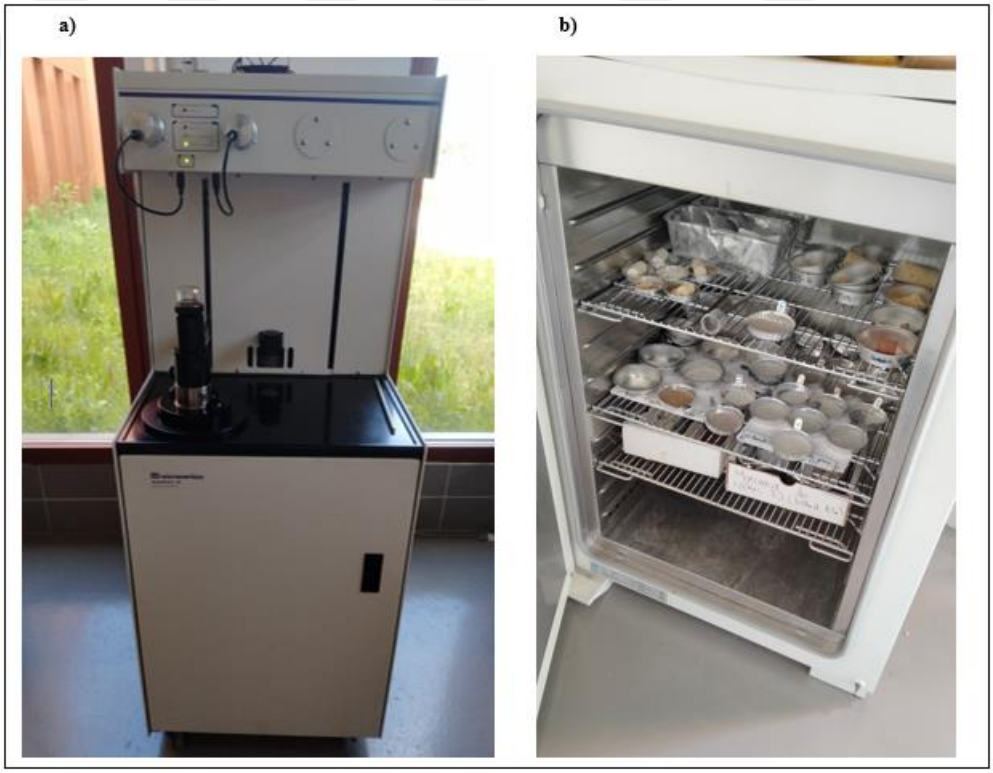

Figure 2.8. a - Micromeritics autopore IV mercury porosimetry instrument b - Mmm medcenter 40 °c sample oven

Micromeritics AutoPore IV Mercury Porosimetry Instrument was used to analyze the samples from microplastic based experiments. In the purpose of having a better understanding on how these particular types microplastics with different concentrations in saturated porous media effects materials porosity, a series of Mercury Intrusion porosimetry analysis were carried out. Changeset on intragranular (within particles) porosity of quartz sand samples which was used in microplastic based transfer column experiments under the different concentration conditions was observed. Each sample was got dry in the 40 °C scientific used oven minimum 24 hours.

3. RESULTS

3.1. Characterization of Nanoplastics Microplastics and Quartz Sands

Size distribution nanoplastics of APS (Amidine Polystyrene), SPS (Sulfate Polystyrene) and SDS coated APS (Sodium Dodecyl Sulfate coated Amidine Polystyrene) NPls was further observed in pure water of 50 mg/l concentrations. NPls particles was observed spherical. Based on TEM image analysis, APS NPls mean particle size was found equal to 152 nm with size range from 4 nm to 175 nm. SPS NPls particle average diameter size was found equal to 104 nm with size range from 12 nm to 128 nm. SDS coated PS NPls particle size averagely was found 163 nm with size range from 39 nm to 186 nm. The size distribution was explained with a TEM image of NPls and its histograms in following figures.(3.1, 3.2, 3.3)

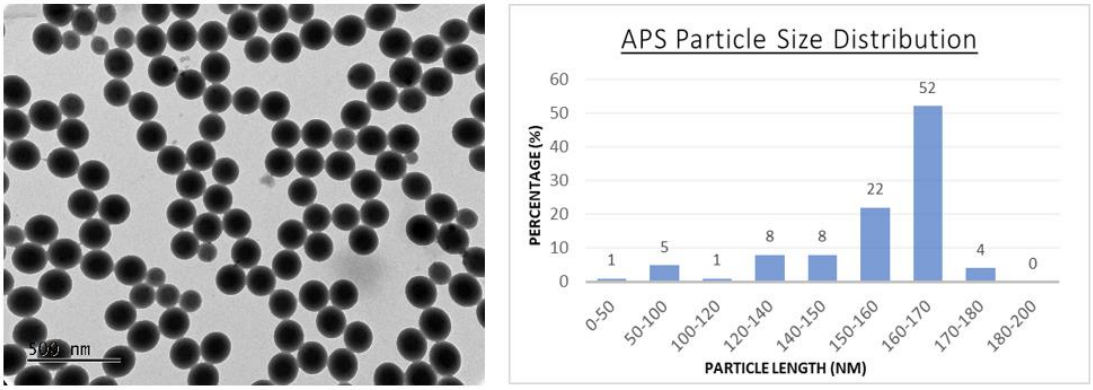

Figure 3.1. Amidine ps npls tem image & particle size distribution

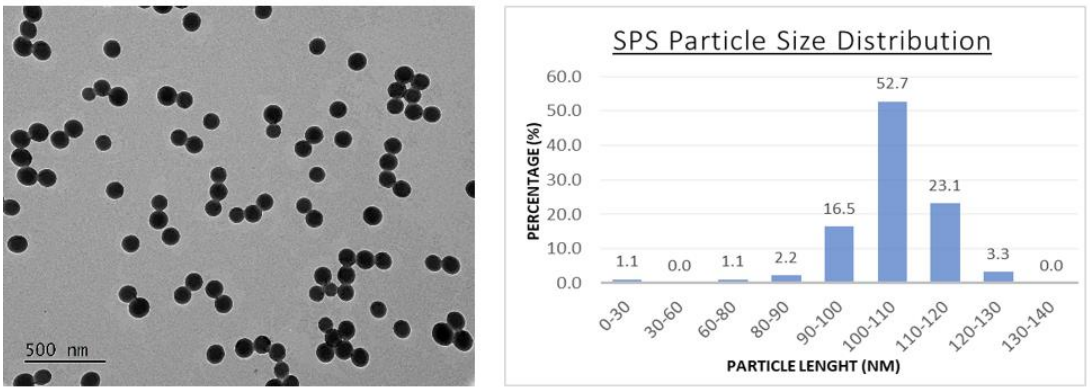

Figure 3.2. Figure 10 Sulfate ps npls tem image & particle size distribution

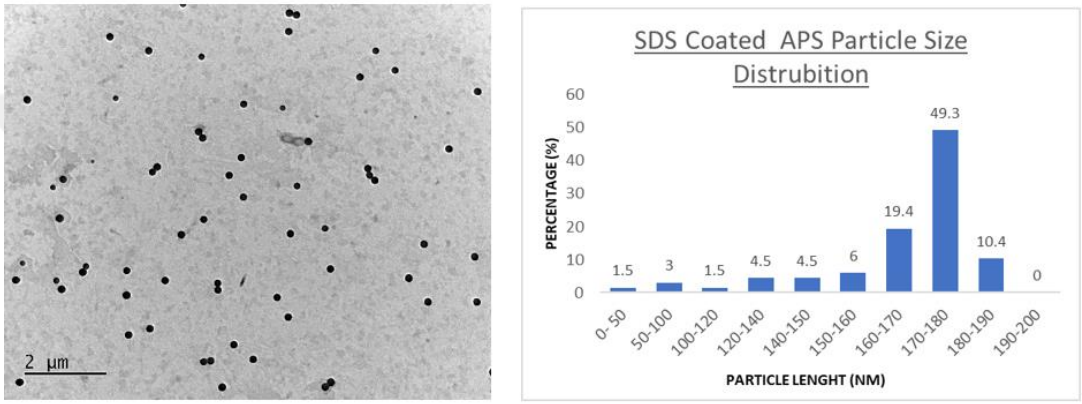

Figure 3.3. Sds coated aps npls tem image & particle size distribution

Statistical calculations of observed different NPls sizes are regrouped in Table 3.1. It appears that size distributions do not follow a perfect Gauss curve. Then it is important to precise the standard deviation of the sizes of the different NPls used to potentially explained difference between theorical behavior and observed one in the 1D model transport.

Table 3.1. Statistical parameters of npls sizes in "nm" scale from tem images

Type of NPls	Size of Population	Min	Max	Mean	Standart Deviation	Median
APS	158	5	173	152	27	162
SPS	91	12	128	104	13	106
SDS	67	39	186	163	28	171

Polyethylene (PE) types MPls particles directly was observed with optical microscopy. Particles was three dimensional and non-spherical. It didn't have a regular-looking shape and varied by grain. Based on optical microscopy image

analysis PE type MPls mean particle size was found nearly 7 µm with size range from 2 µm to 24 µm.

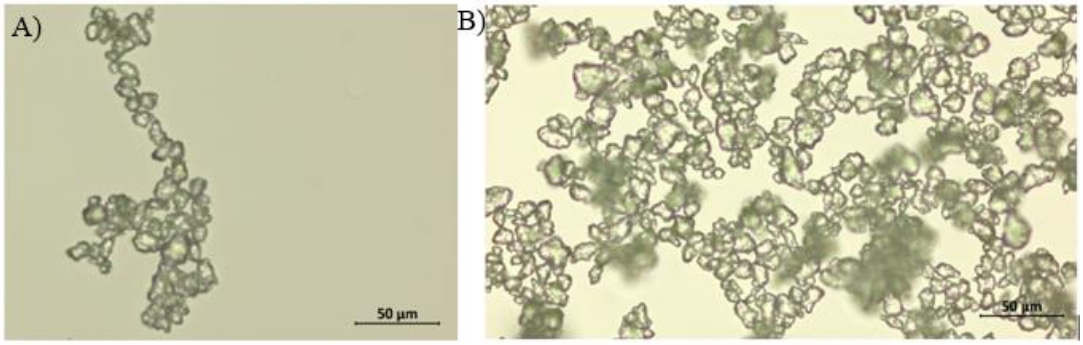

Figure 3.4. Optical microscopic images of pe mpls particles

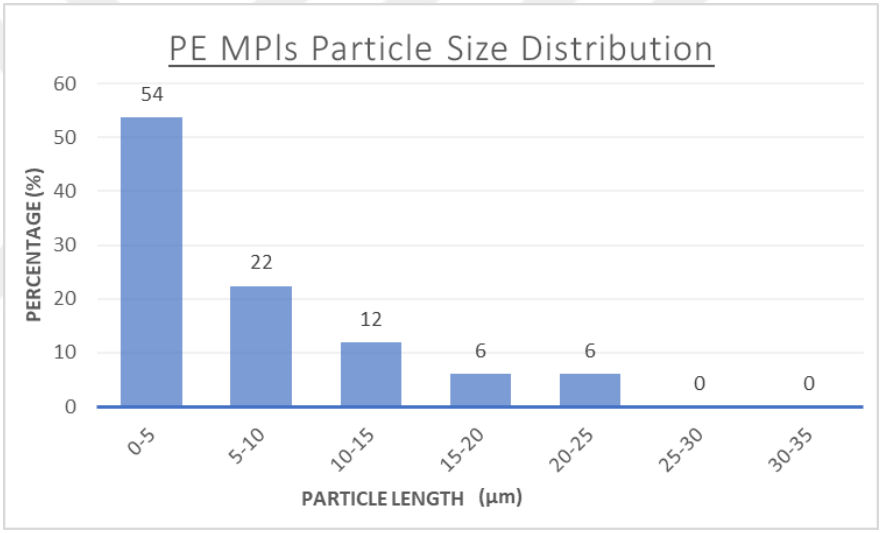

Figure 3.5. Pe mpls particle size distribution

Statistical calculations of measured PE MPls particle sizes can be seen in Table 3.2. Mentioned values were calculated by the Fig. 3.4.A of PE MPls particles image.

Table 3.2. Statistical parameters of pe mpls sizes (µm) by optical microscopy

Type of MPls	Size of Population	Min	Max	Mean	Standart Deviation	Median
PE	68	2	24	7	5	5

The optical microscopy images of MPls reveals a complex distribution of small particles regrouped to form bigger particles and appear as colloids (size between 1 nm to 1 μm and polyelectronic properties). This fact is of great importance to study the transport behavior of such materials.

The characterization of sand samples was observed by SEM at various levels of magnifications to observe surface morphology, texture of raw and affected samples

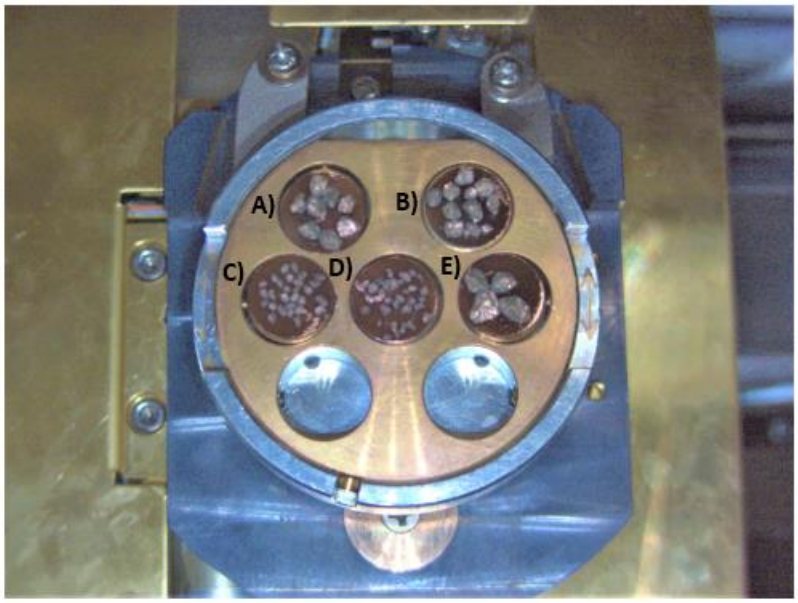

Figure 3.6. Prepared quartz samples for sem observation a) Sample t1 b) Sample t2 c) Sample ga1 d) Sample g2 d) Invalid

It showed that washed, not affected by MPls quartz sand Sample T1 (virgin Turkish quartz sand sample) in Figure 3.7 showed very ordered silica crystals at the surface. The surface's morphology was mostly smooth. Small cracks, relatively mesopores or light roughness was observed on the sand surface.

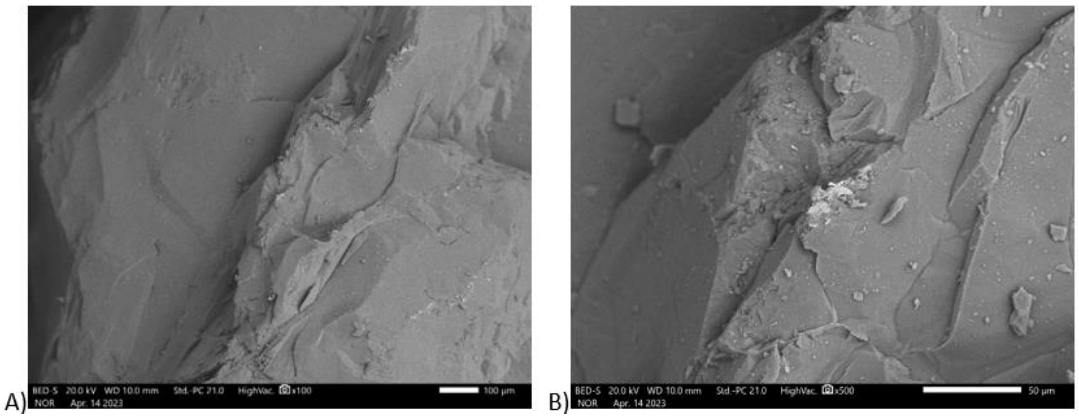

Figure 3.7. Sem images of t1 sand sample surface a - 100µm scale unit b - 50µm scale unit

Comparing the images of virgin sands (Figure 3.7.) and T2 sand sample which affected by 20 mg/l MPls concentration transfer column test with (Figure 3.8.), had not showed significantly different surface than plain sand. It could signify that Turkish sand grain texture was not able to trap MPls.

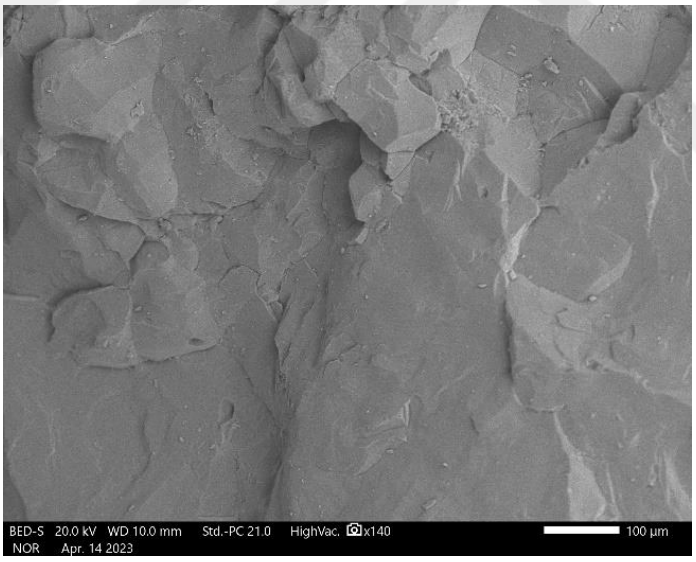

Figure 3.8. Sem images of t2 sand sample surface in 100 µm scale unit

Figure 3.9. was imaged on T2 sand grain surface with smaller scale and it was observed with SEM-EDX (Energy Disperse X-ray Spectroscopy) analysis to see the chemical composition and properties of 5 chosen specific spectra location which can be seen in Figure 3.9. on grain. Analysis results showed that spectra2, spectra4 and spectra5 are quartz sand itself with nearly 99.5% SiO_2 content and spectre1 and spectra3 is just impurities of 5% Al+K and %11 Na+Al content with nearly 95% and

89% SiO_2 on the sand grain. Similarly, Detailed atomic composition diagram can be seen in Appendix-2.

Figure 3.9. Chosen spectra point for sem-edx analysis to determine atomic distribution on t2 sand sample surface

Table 3.3. Sem-edx analysis atomic percentage results of t2 sand sample surface

	Results type			% atomic	
Label of spectra	Spectre 1	Spectre 2	Spectre 3	Spectre 4	Spectre 5
O	65.37	66.62	63.09	66.63	66.65
Na	0	0	4.95	0	0
Mg	0.31	0	0.17	0	0
Al	4.01	0.29	6.27	0.22	0.09
Si	29.21	33.09	25.36	33.15	33.26
S	0	0	0	0	0
Cl	0	0	0	0	0
K	1.02	0	0	0	0
Ca	0	0	0	0	0
Ti	0	0	0	0	0
Fe	0.07	0	0	0	0
Zr	0	0	0.16	0	0
Total	100	100	100	100	100

Geneva sand as a grain has ellipsoidal shape and initial condition grain surface was observed with SEM as it can be seen in Figure 3.10. that their surfaces are not perfectly smooth and may have small cavities comparison to Turkish quartz sand. Also, images shows that the sand surface has rough surface and irregularities which may lead to the place for deposition of NPls particles.

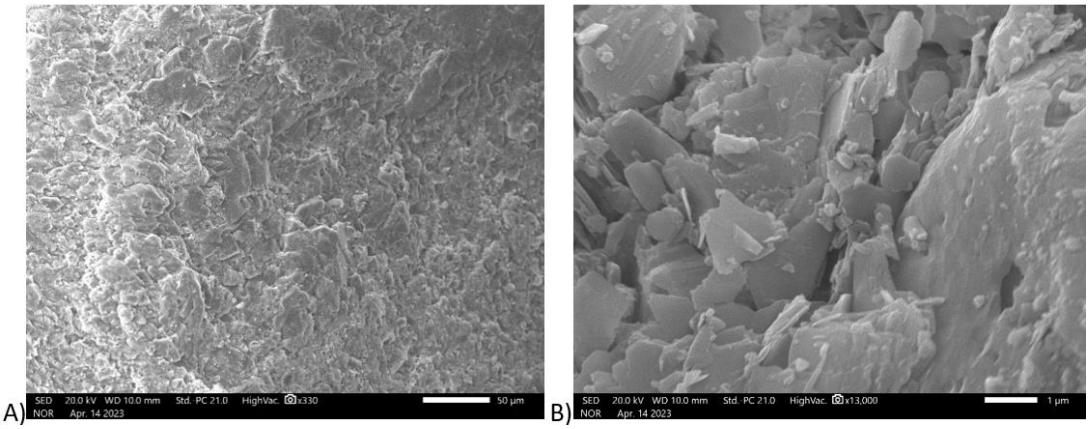

Figure 3.10. Sem images of ga1 sand sample surface b - 50µm scale unit c - 1µm scale unit

SEM images of G2 sand sample which it was used saturated porous media in NPls transfer column test has shown individual NPls presence on the sand surface. It was observed that NPls particles are individually placed (black arrows). and not aggregated but attach to the sand surface as it can be seen in Figure 3.11. This observation means that a fraction of the NPls can be retained by the Geneva sand.

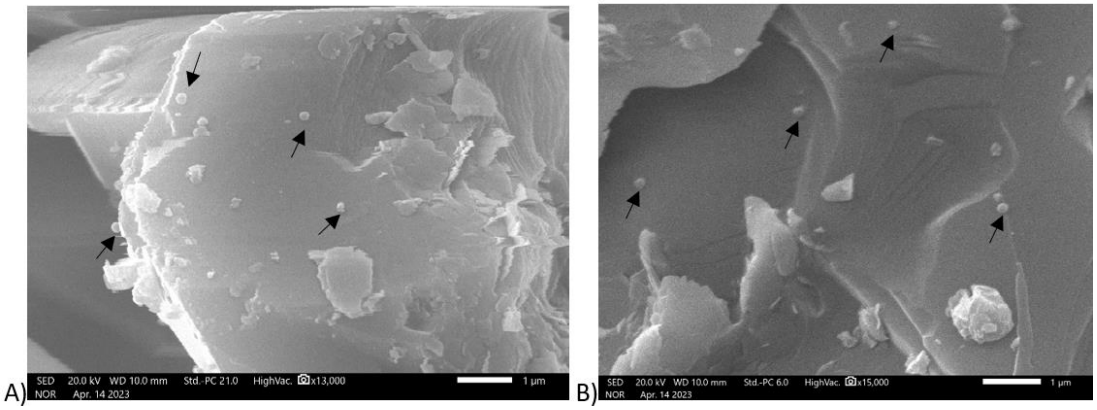

Figure 3.11. Sem images of g2 sand sample surface a - 1µm scale unit b - 1µm scale unit

3.2. Surface Area Analysis and Porosity Measurements

The N_2 BET surface area plots used to evaluate the N_2 BET spesific surface areas of the samples are presented in Table 2. The correlation of the plots was observed linear. The determined specific surface areas of quartz sand sample with different types and concentrated NPls are summarized in Table 3.4. The specific surface areas of sand

samples (determined with BET method) was observed to increase with the increase of the NPls concentrations in saturated porous media. With any type of NPls specific surface areas were observed to increase from initial condition to 100 mg/l to 1000 mg/l concentration. BET method showed that despite the increase of NPls concentration values, determined specific surface area results does not follow a particular sequence. No linearity was observed in the increase.

Table 3.4. Calculated surface area with bet method

Sand Type	Sample Name	Used NPls types in the mixture	Prepared mixture Concentration (mg/l)	Calculated Specific Surface Area (cm^2/g)
Geneva	GA1	-	Raw Sample	530
Geneva	G4	APS	100	680
Geneva	G2	APS	1000	740
Geneva	G7	SPS	100	670
Geneva	G5	SPS	1000	750
Geneva	G10	SDS	100	740
Geneva	G8	SDS	1000	790

The results of specific surface area analysis are shown Table 3.4. The relations of increasing sand samples surface areas with the increase of NPls concentrations on the saturated porous media has shown a correct proportion. The increases of surface area values are not linearly. Virgin sample specific surface area was found 530 cm2/g. Specific surface area of plain sand sample is increased from 530 cm2/g to 680 cm2/g, which is with the injection of 100 mg/l concentration of APS NPls mixtures to saturated porous media. When it was measured Specific surface area of sand sample affected APS NPls of 1000 mg/l concentrated mixtures, it was found 740 cm2/g and it has showed 39% of increase compared to the plain sand sample. Closely to those results, also sand samples affected by SPS NPls has shown increase in specific surface area with 100 mg/l concentration and was found 670 cm2/g with the 26% increase. With the effect of 1000 mg/l concentrated SPS NPls sand samples specific surface area was found 750 cm2/g with the 41% increase from the initial condition. Lastly, the specific surface area of the Geneva sand sample was found to be 740 cm2/g by injection of 100 mg/l concentration under the influence of SDS NPls into the same type of saturated porous medium. The surface area of the Geneva sand sample was found to be 740 cm^2/g by injection of 100 mg/l concentration under the influence of

SDS NPls into the same type of saturated porous medium. Concentration of 1000 mg/l SDS coated PS NPls are affect Geneva sand samples by nearly 49% as a 790 cm^2/g.

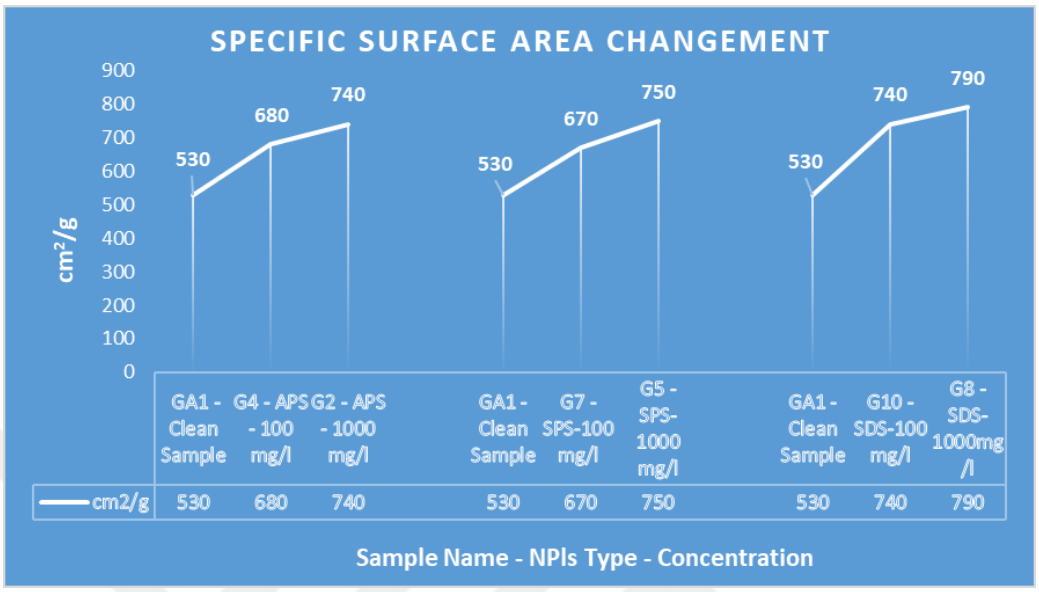

Figure 3.12. Specific surface area changement graph of geneva sand sample which affected by different types of npls on different concentrations

Mercury porosimetry method was applied both Geneva and Turkish types of quartz sand sample. When interpreting the results of the Mercury porosimeter analysis of sand samples, the results were observed in 2 different ways. Firstly, total porosity (%) is in which intraparticle porosity (within particles) and interparticle porosity (between particles) are presented together as indicated in the study of Leon, (1998). Also, Okolo et al., (2015) classified separately in their study, microporosity ($0.3 < dp < 2nm$), mesoporosity ($2 < dp < 50$ nm) and macroporosity ($50 < dp < 60000$ nm) where the dp is pore diameter. So, in order to focus the effect of MPls attached on the sand grain and since the used MPls size was classified between 0 – 30 µm, intraparticle porosity was calculated separate than total porosity. Furthermore, in order to reduce effects of voids between particles (interparticle porosity) and to concentrate intraparticle porosity the effect of pore size diameters greater than 35000 nm was ignored. And only $0 <$ pore diameter < 35000 nm range was investigated. Turturro et al., (2022) indicated that in the mercury intrusion porosimetry analysis used stem volume percentage must be between 25-90% as a range of accuracy of the measurements.

Table 3.5. Calculated porosities (%) with mercury (hg) porosimetry analysis

Microplastics-Based Experiment						
Sample Name	Sample Mass (g)	MPs Type / Injection Concentration (g/L)	Amount of Retained MPls in Saturated Porous Media (%)	Calculated Porosity (%)		Stem Volume Used (%)
				Total	Intraparticle	
GA1	2.7	Clean Sample	0	8.32	0.59	40
GA1 (2^{nd})	3.5	Clean Sample	0	10.36	0.66	59
G12	3.5	PE+surfactant / 10 g/l	72	10.62	0.62	62
G13	3.6	PE+ SDS surfactant / 10 g/l	57	12.29	0.58	73
G11	2.5	PE+surfactant / 20 g/l	51	7.46	0.51	34
T1	3.0	Clean Sample	0	2.27	0.25	11
T2	3.4	PE+surfactant / 20 g/l	13	1.96	0.30	9
T3	3.5	PE+surfactant / 10 g/l	19	2.35	0.39	12

Mercury Intrusion porosimetry experimental data has shown that, as more grains of sand entered the analysis and therefore the analysis according to the sample weight, it was observed that the total porosity changed as the sample mass increased. Sample GA1, Geneva sand, was analysed two different times with different sample mass. With the increase of the sample mass, more grains of sand participating in the analysis. Thus, the change of total porosity by interparticles may outpace the effect of microplastics in porosity of intraparticles.

In the Geneva sand sample, a decrease in the intraparticles porosity of sand which contains microplastics was observed compared to the clean sample. The intraparticles porosity of virgin Geneva sand sample was calculated as 0.66%. It was observed that the same sand sample intraparticles porosity is decreased to the 0.62% under the influence of the 10 g/l of concentration PE MPls with surfactant. 20 mg/l PE MPls with surfactant concentration mixture was dropped the effect more than less concentrated samples to the 0.51% as expected. Intraparticle porosity changement graph according to different types of PE MPls can be seen in Figure 3.13 .

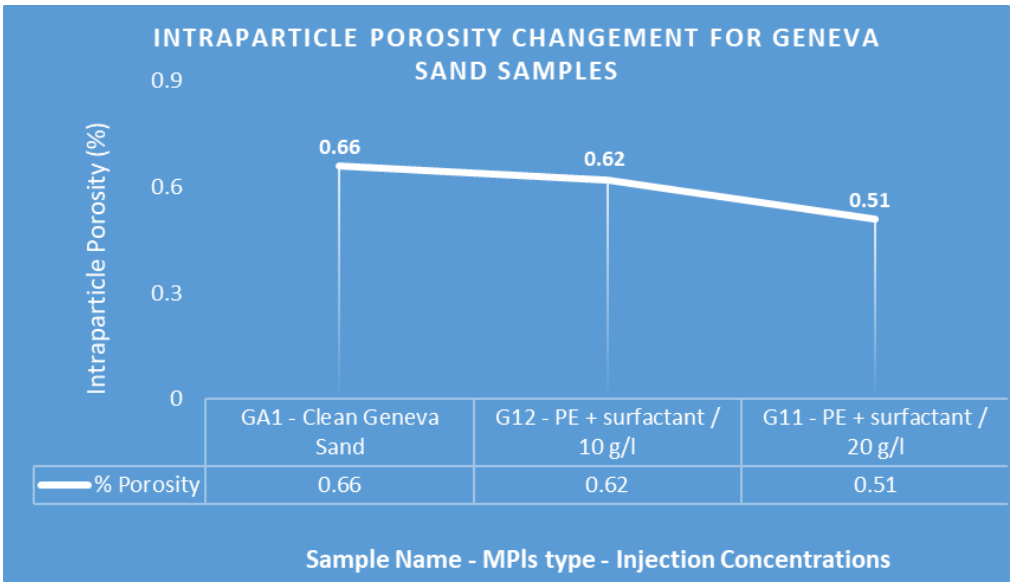

Figure 3.13. Intraparticle porosity changement graph of geneva sand samples with effect of different mpls types and concentrations

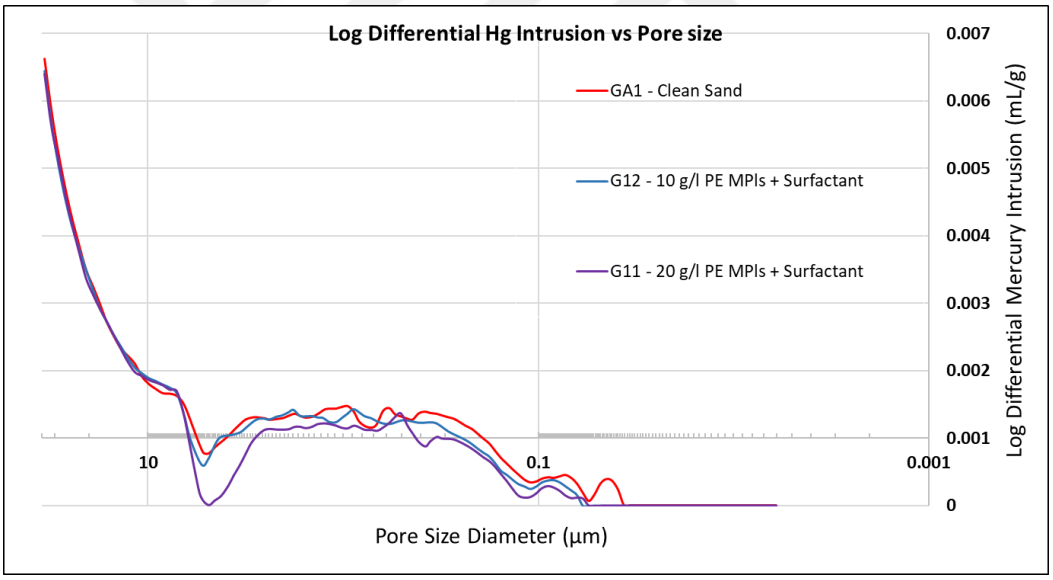

Figure 3.14. Mercury intrusion amount against sand sample pore sizes

Figure 3.14. shows the amount of Mercury intrusion according to different pore size diameters by Mercury porosimetry analysis of Geneva sand samples. It is possible to observe how pore sizes are closing with the related concentration of MPls against to clean Geneva sand sample. For instance, When GA1 sample line compared with G11 sample line, the more Mercury was able to intrude to the pores because pores were more open than contaminated sand sample.

With Turkish quartz sand samples, no reliable results were reached with mercury porosimetry methods. Firstly, stem volume used percentage has observed below the 20% which is the accepted limit according to literature. Also observed results showed unrelated porosity values. Unexpectedly, Porosity of sand samples contaminated by PE MPls has shown higher porosity values than plain sand sample. Furthermore, calculated porosity values of sample contaminated by 20 g/l PE MPls concentration was found higher than sand sample which contaminated by 10 g/l PE MPls concentration.

In order to do a double check and verify the unexpected results 4 different artificial mixture was prepared. The aim was creating a calibration curve of porosity measurements against to different MPls concentration. 10 g Turkish sand sample got fully saturated with 4 ml pure water. Then variable MPls concentration with 1:1 ratio of surfactant (50, 25, 12.5 and 6.25 g/l) was mixed up with Turkish sand. In the end, 10 gr sand samples saturated with 4 ml pure water and contamined with variable MPls concentrations was obtained. Since the smooth and flat surface was observed on the Turkish sand grain surface with the SEM images intragranular porosity was observed with smaller pore size range as between 5 to 10000 nm. Prepared samples and calculated porosity results can be seen in Table 3.6.

Table 3.6. Calibration curve data for hg porosimetry analysis

Sample name	MPls Concentration (g/l)	Analyzed Sample Mass (g)	Calculated Porosity (%)		Stem Volume used (%)
			Total	Intraparticle (5 nm to 10000 nm)	
C1	50	3.5	3.70	0.6	20
C2	25	3.5	4.58	0.72	37
C3	12.5	3.5	6.75	1.11	25
C4	6.25	3.5	6.93	1.78	39

Calculated intraparticles porosity values on Turkish sand with different MPls concentrations graph can be seen below in Figure 3.15.

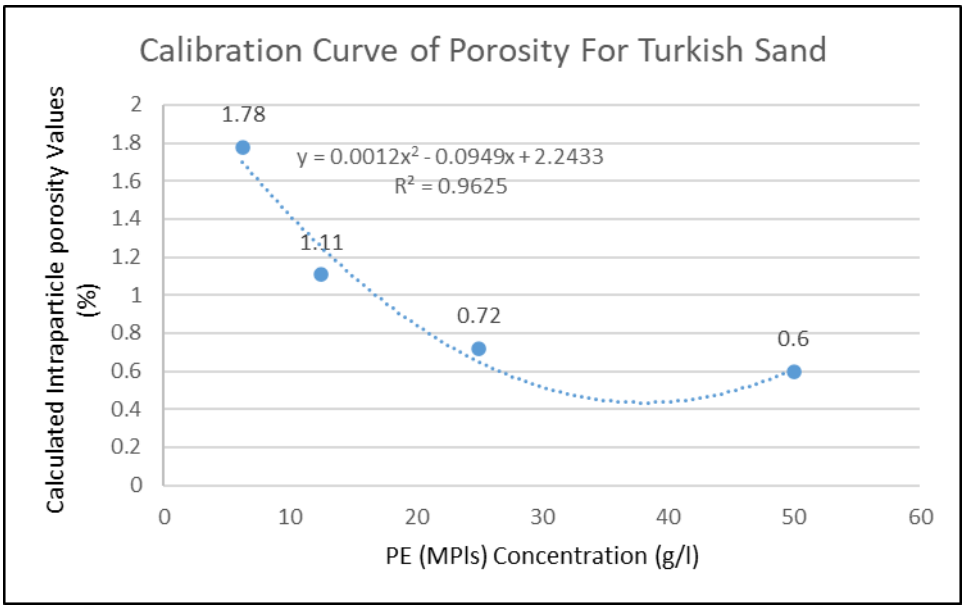

Figure 3.15. Calibration curve graph of turkish sand hg porosimetry analysis

The R^2 was calculated 0.96 was calculated for polinomal curve which is found not accurate for differently concentrated Turkish sand sample with Hg porosimetry measurements results. It was tried to characterize different MPls concentration with linear change of ratio. It was found there is a minor effect of MPls on pores but interparticle porosity overed the intraparticle porosity. And the porosity changement was not observed linearly. The result graphs of Mercury (Hg) log differential intrusion against pore size diameter were shown that calculated intraparticle porosity is not the the intraparticle porosity but still huge void amount between particles. The mentioned graphs can be seen in Appendix 3. The possible reasons for this situation are mentioned in the discussion section.

With X-ray computed tomography method was used to image the arrangement and shape of the pores and then numerical calculations were carried out to determine the porosity of the materials. Sand Sample GA1 and G11, Geneva sand samples, were imaged and observed. The computed tomography was performed with 80 kV and 7W.

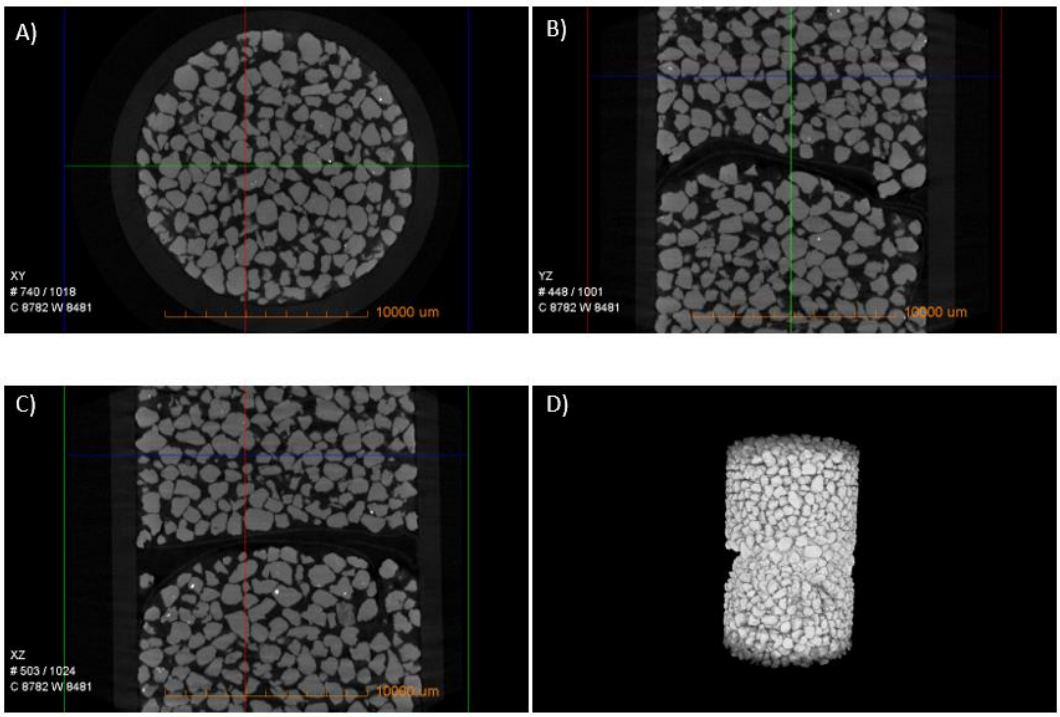

Figure 3.16. X-ray computed tomography imaging of geneva sand sample a - xy axis top view b - yz axis vertical side view c - xz axis vertical side view d - 3d view of imaged sample

In a one sample tube half of it was filled with plain Geneva sand while the other half filled with contaminated Geneva sand sample with 20 g/l PE with surfactant. 2 different scale was used to image same sample. The first used projection scale was 20 µm for pixel. And a total of 1018 projections were made and assembled into 3D model. Second measured scale was 1 pixels for 3.4 µm and a total of 997 projection were made. All parameters such as intensity value or given energy were selected experimentally to ensure to provide best quality of image. After the scanning, the sand grains were determined using the software tools called ImageJ. In order to calculate porosity and separate the grains from voids the threshold was defined in sequenced 2D images. Multiple cross sections of 2D images were merged and void volume and total area calculations were done with 3D stacks. The voids corresponded to the shades of black and the remaining white areas where the sand grains. All pixels corresponding to darker areas and white areas were calculated as area. Also sample tube was define as a limit of area corresponding to total volume (since the sample tube which materials were put to imaging was circular, but images are with the shapes of square so to avoid other spaces not corresponded to the interested sample limits).

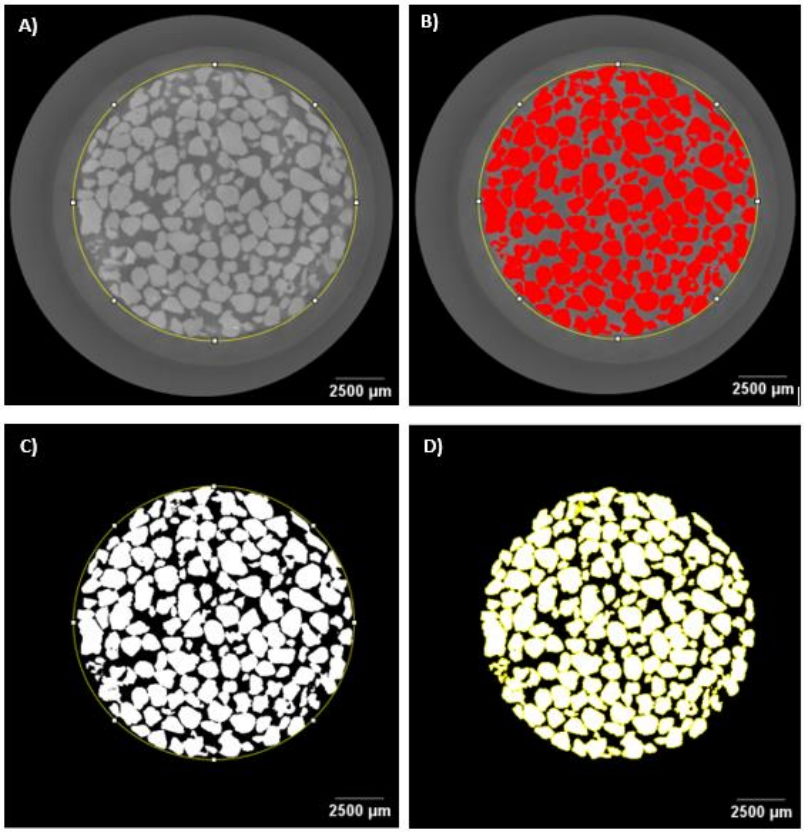

Figure 3.17. Image processing a – 2D top side view of imaged sample with limitation of aoi b - Threshold step to seperation the grains and void c - Thresholded image of sample where white areas sand grains and black areas are void d - Selection of sand grains

The porosity of imaged Geneva sand samples was calculated by finding a difference of total area of interest with total sand grain areas which is equal to total void area and divided that value to total area of interest. The results are multipled by 100 and porosity percentage was calculated. Firstly, more generally imaged calculated. The scale was 20 µm for 1 pixel. Since MPls has sized range between 0-30 µm, MPls could not be found on this scale. Due to high scale, any porosity changement was not expected due to MPls absence since MPls observation could not imaged on that resolution. Geneva raw sand sample and Geneva sand sample which affected by 20 g/l PE MPls was investigated. And the porosity values were found almost same. 68 different raw Geneva sand sample images was merged as sequences and porosity was calculated as 38%. 2D and 3D images can be seen in Fig. 3.18.

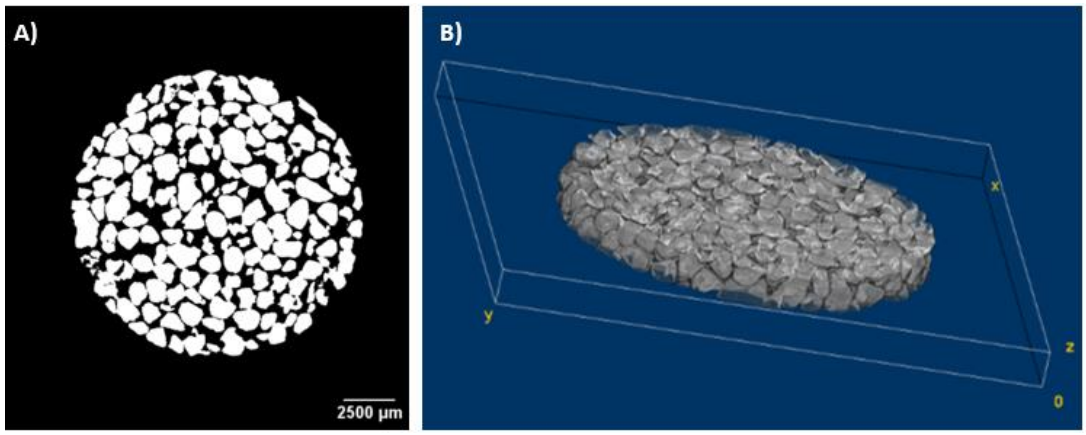

Figure 3.18. Raw geneva sand sample image a – 2D surface top side view b - 3D view of 68 images sequences

271 different contaminated Geneva sand sample images was merged as sequences and porosity was calculated as 37%. 2D and 3D images can be seen in Fig. 3.19.

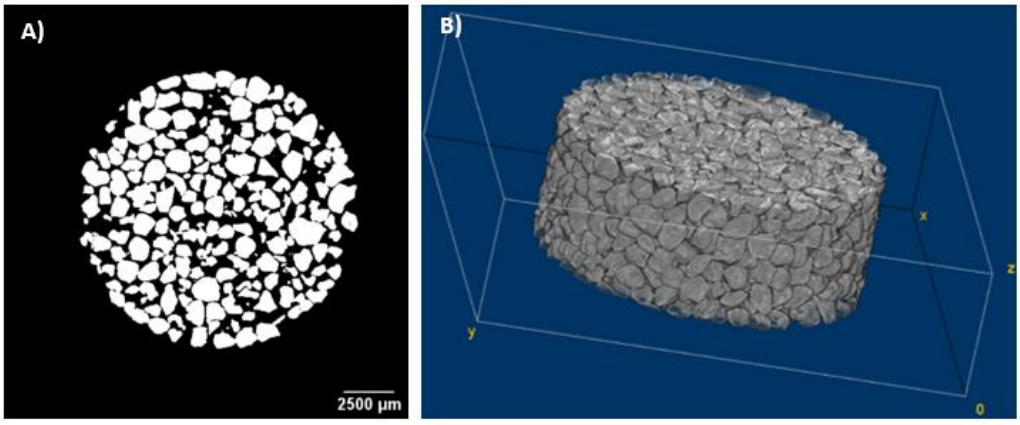

Figure 3.19. Contaminated Geneva sand sample image a – 2D surface top side view – 3D view of 271 images sequences

In order to increase the detail and observe the effect of MPLs contamination on porosity scale got decreased and was set 1 pixels for 3.4 µm. Then same procedure was followed. For raw Geneva sand sample 298 cross section images were sequenced and merged and 3D images were obtained. Under this scale porosity of raw Geneva Sand sample was calculated 39%. 2D and 3D images can be seen in Fig. 3.20.

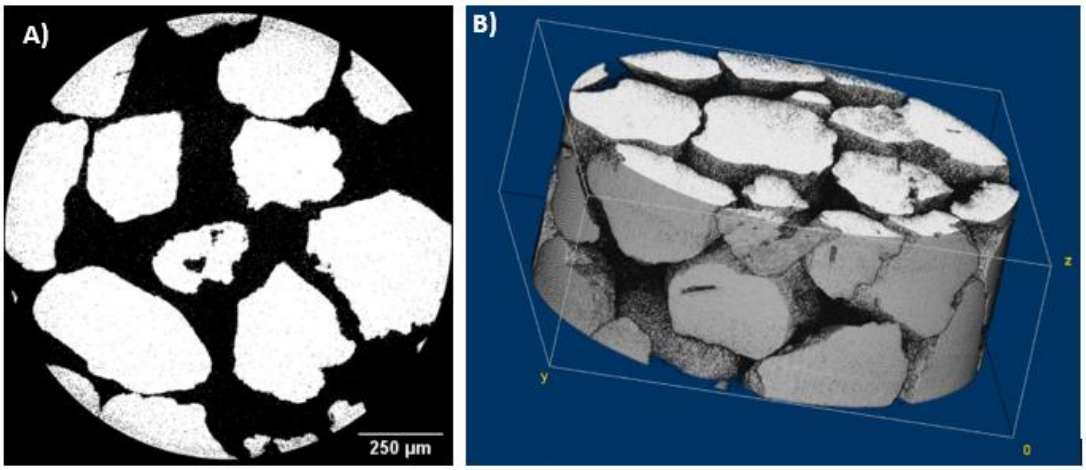

Figure 3.20. Raw Geneva sand sample image with smaller scale a – 2D surface top side view b – 3D view of 298 images sequences

In this scale, also 398 cross section images were sequenced, merged and 3D images were obtained. Under these conditions porosity of contaminated Geneva Sand sample with 20 g/l PE MPls was calculated 35%.

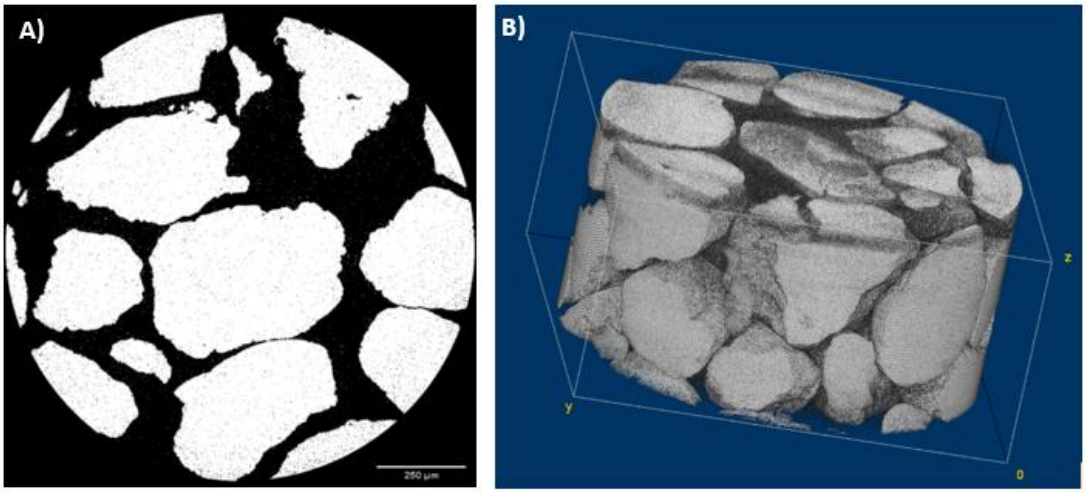

Figure 3.21. Contaminated Geneva sand sample image with smaller scale a - 2D surface top side view b - 3D view of 398 images sequences

Table 3.7. Calculated porosities of geneva sand from sequenced images of x-ray computed tomography

Projection	Sand type	Total Sand Volume (μm^3)	Total Volume (μm^3)	Total void volume (μm^3)	**Porosity (%)**
1 pixel - 20 µm	Raw Geneva	1.31083E+11	2.11435E+11	80352320000	**38**
1 pixel - 20 µm	Contaminated Geneva	5.11623E+11	8.16035E+11	3.04412E+11	**37**
3 pixel - 4 µm	Raw Geneva	434003238	715489507.6	281486270	**39**
3 pixeş - 4 µm	Contaminated Geneva	456206504.3	709465012.2	253258507.9	**35**

Under the lower scale, effect of MPls contamination was observed in terms of porosity. As calculated total porosity decreased 10%.

4. DISCUSSION

Examining the grain size of the MPls and NPls used in the transfer column experiments and imaging grains relationships with each other before they injection into the saturated porous medium was helped to examine the effect on porosity and surface area when they are introduced into the porous media. When NPls mixtures with pure water under the known concentration examined with TEM, images showed that before their injections, these particles were separate from each other. Further, increased specific surface area of sand samples values show the presence of NPls in saturated porous media so they may be attached to sand grain surface individually. SEM images of the sand grain surfaces showed that both of Turkish and Geneva quartz sands has not much porous surface. It was thought that this surface texture may made it difficult for the plastic particles to be attached.

On SEM images MPls particles were not detected on the contaminated Turkish sand grain surface. Very limited number of sand samples were imaged and the possibility of microplastic not being present on that examined particular sand grains at the relevant concentration was considered.

The Hg porosimetry measurement results were found unreliable with Turkish sand sample. The reason for that result might be the texture of nonporous, mostly smooth surface of quartz sand as observed in SEM images of grain surface. Since practically there is no pore in the sample so mercury was able to find no pores when it intrudes to the penetrometer in the experimental setup but could only measure the void between the particles. Furthermore, void volume can be varied with the position of the sand grains. Since sand samples has not a one particular size but size range between 1.2 to 2.4 mm, it may also affect the space volume because of the density of sample in penetrometer and it may increase or decrease space volume so effect the calculated total porosity values. It was also proved that increase of measured sample mass has effect on total porosity with Hg porosimetry method. This might be linked also with total void volume. Also, since the Mercury is destructive method for analyzed sample and the method applying really high pressure to sample so it may affect the attached

MPls in sample since there is not many pores on the sand grain. MPls to the penetrometer (which is sample cup which contains sand sample inside) So it was decided that Mercury intrusion porosimetry is not suitable for this kind of material. Since Geneva sand sample grain surface was observed rougher. Differently, as an additional complimentary analysis in order to do comparison between intraparticle porosity changeset with the effect of different type of surfactant under the same concentration of NPls, sample G13 was analyzed. Intraparticle porosity of G13 was calculated 0.58% under the effect of 10 g/l PE SDS surfactant which was found %6 less than GA1. That result was not added to the comparison graph since there is no parameter to do a comparison. Created calibration curve for Turkish sand sample intraparticle porosity was limited with the range of 5 to 10000 nm. Since any porous surface was not observed, it was aimed to reduce the interparticle porosity. But result graphs which it can seen in Appendix 3, calculated huge amount of Hg intrusion in big pore size which is still could accept as a interparticle void. Furthermore, since the MPls concentration was increased linearly, the porosity was expected to decrease and effect linearly but the measurement technique was not suitable for that kind of material because of texture. Overall, calculated intraparticule porosity values were found really low because of nonporous textures of sand samples and its makes hard to show difference.

X-ray computed tomography methods was used with the projection of 20 µm for pixels. Since MPls studied in this work has a size range between 0 – 25 µm and nearly 88% of MPls has size smaller than 20 µm microplastics was not possible to observe with the method. When projection scale got lower as 3 pixels for 4 µm MPls effects on porosity was observed. According to size of detected MPls in Figure 13, it would be possible to expect more effect of MPls on the porosity changeset if it would be done with lower scale projection than 4 µm.

Bet surface area analyzer can be considered good technique to analyze surface area with N_2 gases. Because nitrogen has a high purity and it can have strong interaction with most solids. Hg intrusion porosimetry can be considered as a not effective way to do the observation of effect MPls and NPls in the terms of porosity on granular sand samples who has not much porous texture since its applied with high pressure and destructive method. In the further studies porosity changeset can tested with physical gas adsorption (physisorption) with the materials which has higher specific surface

areas (>1 m^2/g). Because while gas adsorption is used to analyse smaller pores, Hg (mercury) porosimetry is particularly applicable to porous materials exhibiting larger pores. Since the specific surface areas of used sand materials was <1 m^2/g sensitive methods could not be obtained. Using Kryton for surface area analysis would be more proper method to use since krypton needs less specific surface area to do measurements.

5. CONCLUSION

In this study, the effect of MPls and NPls in 2 different kinds of saturated porous media in the terms of porosity and surface area changement was investigated using variety of complementary experimental methods on the sand samples which was used in plastics transport column experiments. Effect of well characterized NPls as well as not well characterized MPls (according to shape, size range similarities, defined diameters) was investigated.

Imaging methods with SEM, transmission electron microscopy and X-ray computed tomography has applied to the observed materials. TEM imaging observations revealed that NPls particles were individually in the mixture of pure water before the injection of it to the saturated porous media. SEM imaging observations revealed that Geneva sand sample grain has not a smooth surface, and contains small cavities, rough surface and irregularities while Turkish sand sample grain surface was observed as mostly smooth, contains light roughness. Further SEM images showed individual NPls attached to the contaminated Geneva sand surface thus confirming the surface area changement of sand samples. With X-ray computed tomography imaging methods arrangement of grains was visualized with 3D. Closely to Hg porosimetry method of same Geneva sand sample porosity changeset (which was calculated %16 decrease), 10% of difference was observe in porosity changeset between raw Geneva sand sample and contaminated Geneva sand sample with MPls.

BET surface area analysis was revealed that injected concentration of NPls to saturated porous media has directly affect on surface area changeset on the materials. The calculations were shown that 100 mg/l concentrated pure water-NPls mixtures increased surface areas of materials up to 26% while 1000 mg/l pure water-NPls mixtures increased surface area of materials up to 41% compared to initial condition.

Mercury (Hg) intrusion porosimetry method was applied to both Geneva and Turkish quartz sand samples which affected by different concentrations of MPls. The intraparticles porosity changement values of samples related to the injection concentration of NPls was proven. 10 g/l concentrated pure water-PE MPls mixtures

got decreased intraparticle porosity of Geneva sand sample up to 12% where 20 g/l concentrated pure water- PE MPls mixtures has intraparticle porosity decrease was found nearly 22% compared to the initial condition.

In this study it was aimed to explore the porosity changeset between the limit of minimum and maximum limit with small grain particles (Geneva sand) with NPls and bigger sand grain size (Turkish sand) with MPls. The results which obtained from BET surface area analysis and Hg porosimetry can be expected to provide more information about the effect of these kind of plastics in the real nature porous media regarding decrease the infiltration amount of surface water to the aquifers with the reducing effect of porosity,

REFERENCES

Ahamada Rachid, N., & Doğruöz Güngör, N. (2020). Microplastics In Our Planet: Source, Distribution, Effects And Biodegradation. Eskişehir Teknik Üniversitesi Bilim Ve Teknoloji Dergisi - C Yaşam Bilimleri Ve Biyoteknoloji, 9(2), 284–303. Https://Doi.Org/10.18036/Estubtdc.656857

Alshehrei, F. (2017). Biodegradation Of Synthetic And Natural Plastic By Microorganisms. Journal Of Applied & Environmental Microbiology, 5(1), 8–19. Https://Doi.Org/10.12691/Jaem-5-1-2

Brame, J., & Griggs, C. (2016). Surface Area Analysis Using The Brunauer-Emmett-Teller (Bet) Method Scientific Operating Procedure Series: Sop-C Environmental Laboratory. Www.Erdc.Usace.Army.Mil.

Brantley, S., & Mellott, N. (2022). Surface Area And Porosity Of Silicates.

Bulcke, J. Van Den, Boone, M., Acker, J. Van, Stevens, M., & Hoorebeke, L. Van. (2009). X-Ray Tomography As A Tool For Detailed Anatomical Analysis. Annals Of Forest Science, 66(5), 508–508. Https://Doi.Org/10.1051/Forest/2009033

Chia, R. W., Lee, J. Y., Kim, H., & Jang, J. (2021). Microplastic Pollution In Soil And Groundwater: A Review. In Environmental Chemistry Letters (Vol. 19, Issue 6, Pp. 4211–4224). Springer Science And Business Media Deutschland Gmbh. Https://Doi.Org/10.1007/S10311-021-01297-6

Dong, H., Zhang, H., Zuo, Y., Gao, P., & Ye, G. (2018). Relationship Between The Size Of The Samples And The Interpretation Of The Mercury Intrusion Results Of An Artificial Sandstone. Materials, 11(2). Https://Doi.Org/10.3390/Ma11020201

Egerton, R. F. (2005). Physical Principles Of Electron Microscopy : An Introduction To Tem, Sem And Aem. Springer.

Goldstein, J. I., Newbury, D. E., Echlin, P., Joy, D. C., Lyman, C. E., Lifshin, E., Sawyer, L., & Michael, J. R. (2003). Scanning Electron Microscopy And X-Ray Microanalysis. Springer Us. Https://Doi.Org/10.1007/978-1-4615-0215-9

Han, R., Zou, W., Zhang, Z., Shi, J., & Yang, J. (2006). Removal Of Copper(Ii) And Lead(Ii) From Aqueous Solution By Manganese Oxide Coated Sand. I. Characterization And Kinetic Study. Journal Of Hazardous Materials, 137(1), 384–395. Https://Doi.Org/10.1016/J.Jhazmat.2006.02.021

He, L., Wu, D., Rong, H., Li, M., Tong, M., & Kim, H. (2018). Influence Of Nano- And Microplastic Particles On The Transport And Deposition Behaviors Of Bacteria In Quartz Sand. Environmental Science And Technology, 52(20), 11555–11563. Https://Doi.Org/10.1021/Acs.Est.8b01673

Hlaváč, D., Tokarský, J., Kulhánková, L., Matějka, V., & Čapková, P. (2014). Molecular Modeling Study Of Polyaniline Thin Film Formation On Glass Substrate. Advanced Science, Engineering And Medicine, 6(4), 468–472. Https://Doi.Org/10.1166/Asem.2014.1522

Hu, E., Yuan, H., Du, Y., & Chen, X. (2021). Ldpe And Hdpe Microplastics Differently Affect The Transport Of Tetracycline In Saturated Porous Media. Materials, 14(7). Https://Doi.Org/10.3390/Ma14071757

Hul, G., Ramseier Gentile, S., Zimmermann, S., & Stoll, S. (2022). Towards A Better Understanding Of Ceo2 Manufactured Nanoparticles Adsorption Onto Sand Grains Used In Drinking Water Treatment Plants. Colloids And Surfaces A: Physicochemical And Engineering Aspects, 646. Https://Doi.Org/10.1016/J.Colsurfa.2022.129000

Imaging Center Bordeaux. (N.D.). Operating Manual Transmission Electron Microscope Hitachi H7650.

Klobes, P., Riesemier, H., Meyer, K., Goebbels, J., & Hellmuth, H. (1997). Rock Porosity Determination By Combination Of X-Ray Computerized Tomography With Mercury Porosimetry.

Leon, C. A. (1998). New Perspectives In Mercury Porosimetry.

Macleod, M., Peter, H., Arp, H., Tekman, M. B., & Jahnke, A. (2021). The Global Threat From Plastic Pollution.

Maire, E., & Withers, P. J. (2014). Quantitative X-Ray Tomography. In International Materials Reviews (Vol. 59, Issue 1, Pp. 1–43). Https://Doi.Org/10.1179/1743280413y.0000000023

Mariano, S., Tacconi, S., Fidaleo, M., Rossi, M., & Dini, L. (2021a). Micro And Nanoplastics Identification: Classic Methods And Innovative Detection Techniques. Frontiers In Toxicology, 3. Https://Doi.Org/10.3389/Ftox.2021.636640

Mariano, S., Tacconi, S., Fidaleo, M., Rossi, M., & Dini, L. (2021b). Micro And Nanoplastics Identification: Classic Methods And Innovative Detection Techniques. Frontiers In Toxicology, 3. Https://Doi.Org/10.3389/Ftox.2021.636640

Mcdevitt, J. P., Criddle, C. S., Morse, M., Hale, R. C., Bott, C. B., & Rochman, C. M. (2017). Addressing The Issue Of Microplastics In The Wake Of The Microbead-Free Waters Act - A New Standard Can Facilitate Improved Policy. Environmental Science And Technology, 51(12), 6611–6617. Https://Doi.Org/10.1021/Acs.Est.6b05812

Mohammed, A., & Abdullah, A. (2018). Scanning Electron Microscopy (Sem): A Review.

Okolo, G. N., Everson, R. C., Neomagus, H. W. J. P., Roberts, M. J., & Sakurovs, R. (2015). Comparing The Porosity And Surface Areas Of Coal As Measured By Gas Adsorption, Mercury Intrusion And Saxs Techniques. Fuel, 141, 293–304. Https://Doi.Org/10.1016/J.Fuel.2014.10.046

Okutan, H. M., Sağir, Ç., Fontaine, C., Nauleau, B., Kurtulus, B., Le Coustumer, P., & Razack, M. (2022). One-Dimensional Experimental Investigation Of Polyethylene Microplastic Transport In A Homogeneous Saturated Medium. Frontiers In Environmental Science, 10. Https://Doi.Org/10.3389/Fenvs.2022.885875

Qiming, W., & Qinhong, H. (2019). Using Mercury Intrusion Porosimetry To Identifying The Sample Size Effecton Pore Structure Characteristics Of The Eagle Ford Shale. Search And Discovery Article - The University Of Texas At Arlington, 11, 1184–1190. Https://Doi.Org/10.1306/42373wang2019

Raja, P. M. V, & Barron, A. R. (2022). Physical Methods In Chemistry And Nano Science. Https://Libretexts.Org

Ramirez Arenas, L., Ramseier Gentile, S., Zimmermann, S., & Stoll, S. (2022). Fate And Removal Efficiency Of Polystyrene Nanoplastics In A Pilot Drinking Water Treatment Plant. Science Of The Total Environment, 813. Https://Doi.Org/10.1016/J.Scitotenv.2021.152623

Rigby, S. P., & Edler, K. J. (2002). The Influence Of Mercury Contact Angle, Surface Tension, And Retraction Mechanism On The Interpretation Of Mercury Porosimetry Data. Journal Of Colloid And Interface Science, 250(1), 175–190. Https://Doi.Org/10.1006/Jcis.2002.8286

Salvo, L., Suéry, M., Marmottant, A., Limodin, N., & Bernard, D. (2010). 3d Imaging In Material Science: Application Of X-Ray Tomography. In Comptes Rendus Physique (Vol. 11, Issues 9–10, Pp. 641–649). Elsevier Masson Sas. Https://Doi.Org/10.1016/J.Crhy.2010.12.003

Schlumberger, C., & Thommes, M. (2021). Characterization Of Hierarchically Ordered Porous Materials By Physisorption And Mercury Porosimetry. In Advanced Materials Interfaces (Vol. 8, Issue 4). Wiley-Vch Verlag. Https://Doi.Org/10.1002/Admi.202002181

Stepien, A., Durlej, M., & Skowera, K. (2022). Application Of The Computed Tomography Method For The Evaluation Of Porosity Of Autoclaved Materials. Materials, 15(23). Https://Doi.Org/10.3390/Ma15238472

Turturro, A. C., Caputo, M. C., & Gerke, H. H. (2022). Mercury Intrusion Porosimetry And Centrifuge Methods For Extended-Range Retention Curves Of Soil And Porous Rock Samples. Vadose Zone Journal, 21(1). Https://Doi.Org/10.1002/Vzj2.20176

Williams, D. B. (David B., & Carter, C. Barry. (2009). Transmission Electron Microscopy : A Textbook For Materials Science. Springer.

Windsor, F. M., Durance, I., Horton, A. A., Thompson, R. C., Tyler, C. R., & Ormerod, S. J. (2019). A Catchment-Scale Perspective Of Plastic Pollution. In Global Change Biology (Vol. 25, Issue 4, Pp. 1207–1221). Blackwell Publishing Ltd. Https://Doi.Org/10.1111/Gcb.14572

Yee, M. S. L., Hii, L. W., Looi, C. K., Lim, W. M., Wong, S. F., Kok, Y. Y., Tan, B. K., Wong, C. Y., & Leong, C. O. (2021). Impact Of Microplastics And Nanoplastics On Human Health. In Nanomaterials (Vol. 11, Issue 2, Pp. 1–23). Mdpi Ag. Https://Doi.Org/10.3390/Nano11020496

Yu, Y., & Flury, M. (2021). Current Understanding Of Subsurface Transport Of Micro- And Nanoplastics In Soil. Vadose Zone Journal, 20(2). Https://Doi.Org/10.1002/Vzj2.20108

APPENDICES

Appendix A. Geneva sand grains characteristics provided by the manufacturer.

Grain size (mm)	Volume proportion of particles in the range (%)	Cumulative distribution (%)	Sphericity	Aspect ratio	Convexity
0 - 0.75	0.05	0.05	0.785	0.660	0.979
0.75 – 1	0.00	0.05	0.806	0.581	0.992
1 – 1.2	0.01	0.06	0.567	0.328	0.979
1.2 – 1.5	0.07	0.13	0.577	0.310	0.982
1.5 – 2	1.54	1.67	0.708	0.437	0.986
2 – 2.38	7.26	8.93	0.774	0.529	0.988
2.38 – 2.83	24.74	33.67	0.823	0.622	0.989
2.83 – 3.36	40.64	74.31	0.845	0.692	0.989
3.36 – 4	22.98	97.29	0.848	0.728	0.987
4 – 4.76	2.67	99.96	0.826	0.761	0.982
> 4.76	0.04	100	0.654	0.742	0.956

Appendix B. SEM-EDX analysis Turkish sand atomic composition diagram of 5 spectra

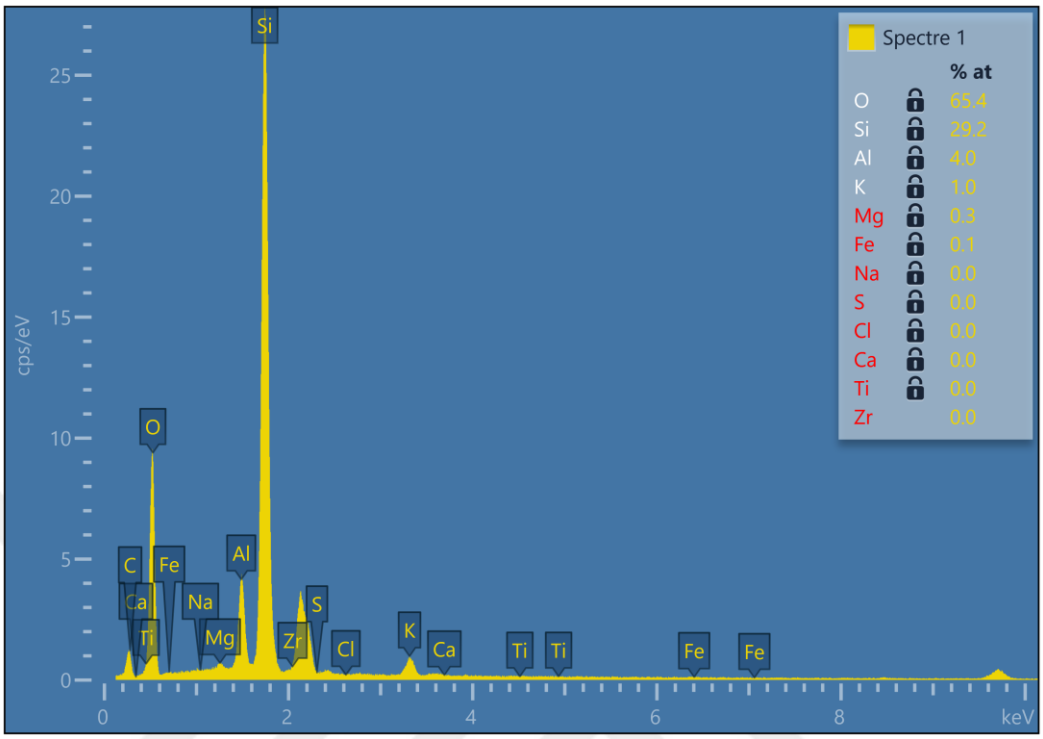

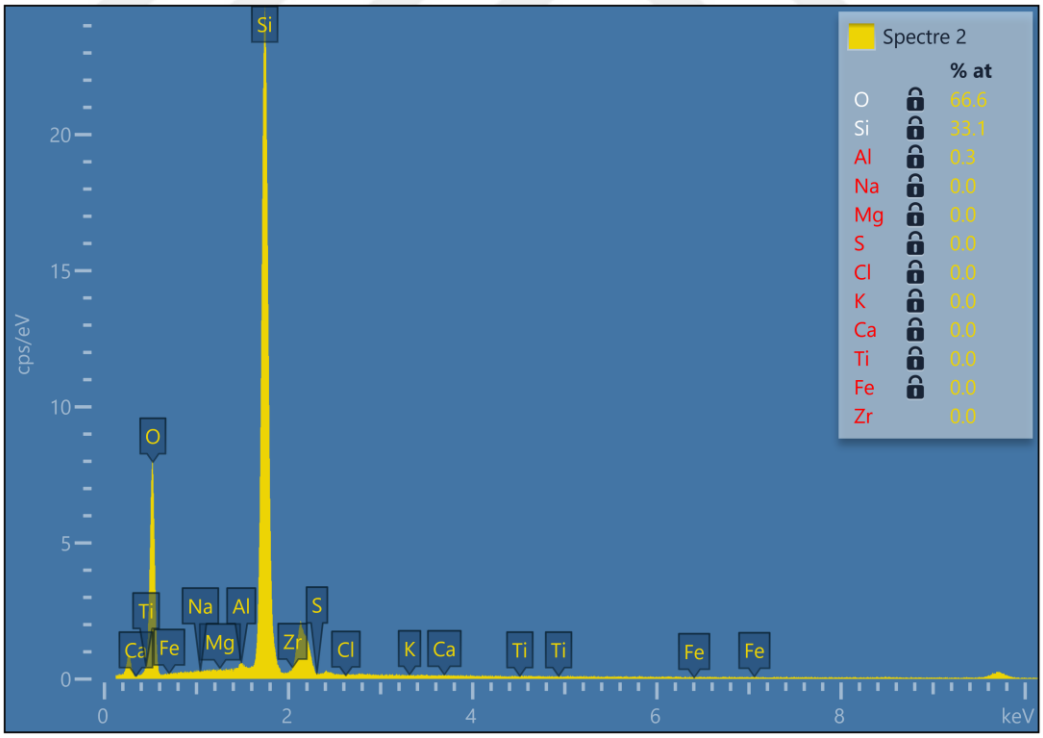

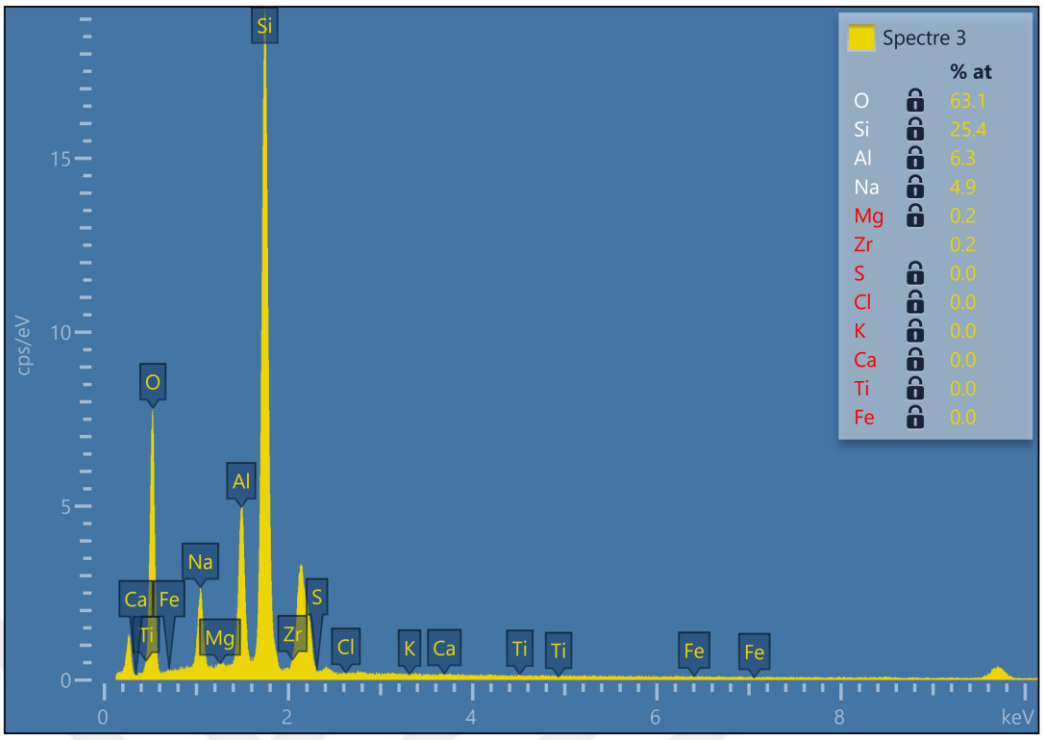
Spectre 3
% at
O 63.1
Si 25.4
Al 6.3
Na 4.9
Mg 0.2
Zr 0.2
S 0.0
Cl 0.0
K 0.0
Ca 0.0
Ti 0.0
Fe 0.0
cps/eV
keV
Si
O
Al
Na
Ca
Fe
Ti
Mg
Zr
S
Cl
K
Ca
Ti
Ti
Fe
Fe

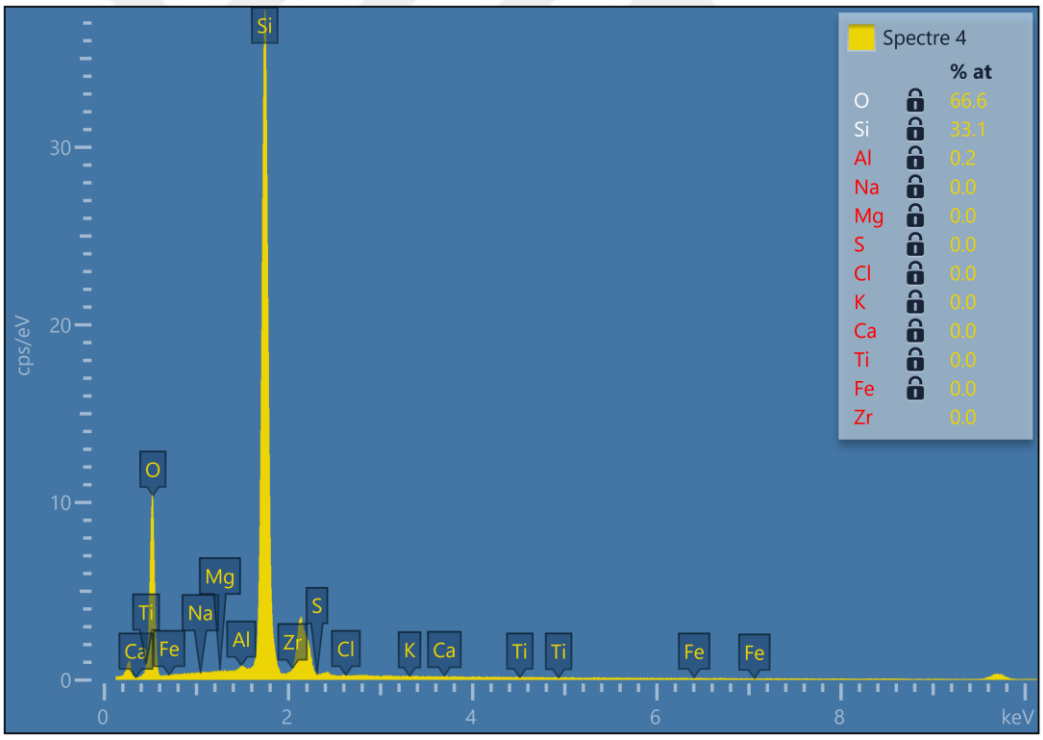
Spectre 4
% at
O 66.6
Si 33.1
Al 0.2
Na 0.0
Mg 0.0
S 0.0
Cl 0.0
K 0.0
Ca 0.0
Ti 0.0
Fe 0.0
Zr 0.0
cps/eV
keV
Si
O
Mg
Ti
Na
Ca
Fe
Al
Zr
S
Cl
K
Ca
Ti
Ti
Fe
Fe

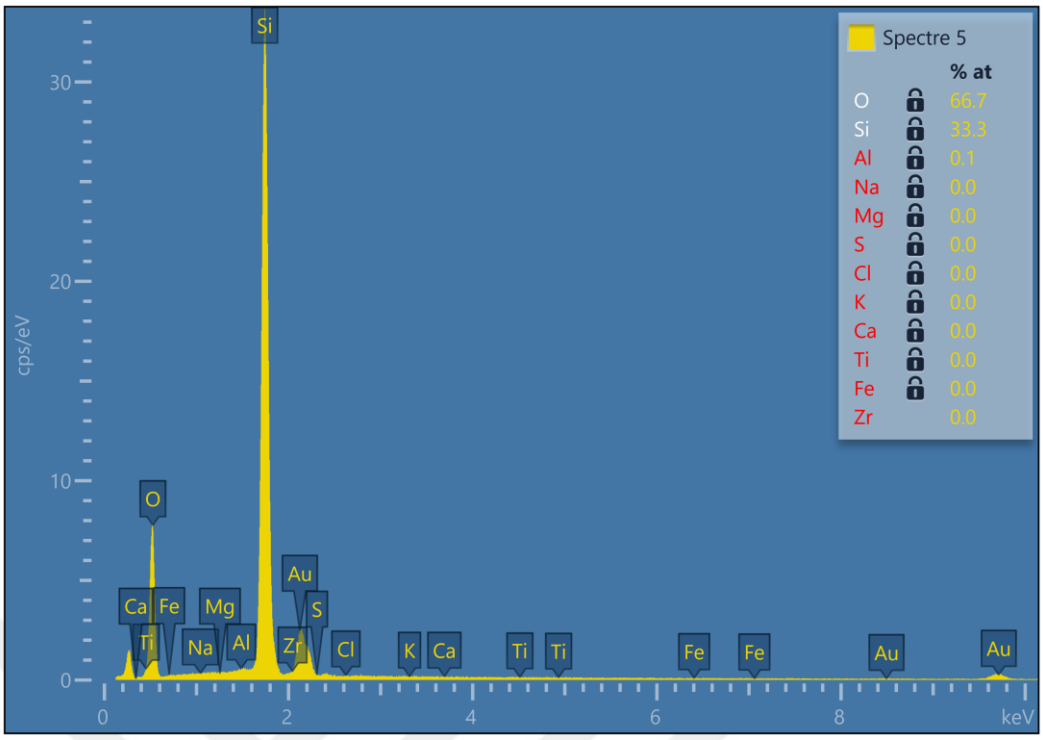
Spectre 5
% at
O 66.7
Si 33.3
Al 0.1
Na 0.0
Mg 0.0
S 0.0
Cl 0.0
K 0.0
Ca 0.0
Ti 0.0
Fe 0.0
Zr 0.0
cps/eV
keV
Si
O
Au
Ca
Fe
Mg
S
Ti
Na
Al
Zr
Cl
K
Ca
Ti
Ti
Fe
Fe
Au
Au

Appendix C : Geneva sand sample particle size range analysis

Size of population	Calculated grain size (mm)	
	minimum	maximum
100	0.31	1.44

Grain size (mm)	Volume proportion of particles in the range (%)
0 - 0.5	7
0.5 - 1	68
1 - 1.45	25

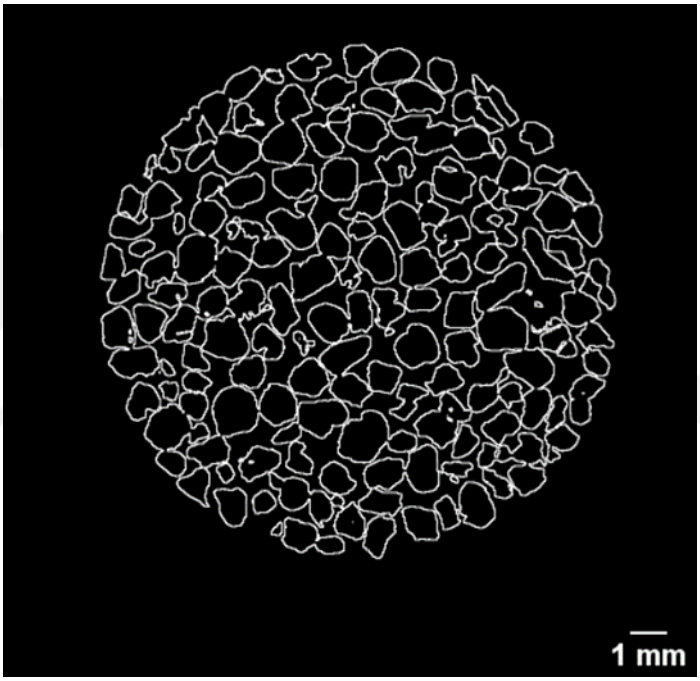

CURRICULUM VITAE

S***** O***

E-mail : s*******@gmail.com

Education

2022 – 2023 M.Sc in Water and Environmental Sciences, Pascal Paoli University of Corsica (France)

2021 – 2023 M.Sc. in Department of Geological Engineering, Mugla Sitki Kocman University, Mugla (Turkey)

September 2017 – February 2018 Erasmus+ Study Mobility, University of Basilicata, Potenza (Italy)

2014 – 2020 – B.Sc in Department of Geological Engineering Programme of Hydrogeology Engineering, Hacettepe University, Ankara (Turkey)

Internships and Professional Experiences

February 2023 – June 2023 Master 2 Intern, Bordeaux Imaging Center, Bordeaux (France)

May 2022 – July 2023 Erasmus+ Trainee, National Laboratory for Civil Engineering (LNEC), Lisbon (Portugal)

June 2021 – August 2022 Junior Consultant Hydrogeologist, PAO Consulting, Ankara (Turkey)